DEFRA/Environment Agency
Flood and Coastal Defence R&D Programme

Reducing Uncertainty in River Flood Conveyance

Interim Report 2: Review of Methods for Estimating Conveyance

Project W5A - 057
March 2003

DEFRA
Department for
Environment,
Food & Rural Affairs

ENVIRONMENT AGENCY

DEFRA / Environment Agency
Flood and Coastal Defence R&D Programme

Review of Methods for Estimating Conveyance

Interim Report 2

DEFRA
Flood Management Division
Ergon House
17 Smith Square
London SW1P 3JR

and

Science Directorate
Cromwell House
Dean Stanley Street
London SW1P 3JH

Environment Agency
Rio House
Waterside Drive
Aztec West
Almondsbury
Bristol BS32 4UD

November 2002

Publishing organisation

Environment Agency
Rio House
Waterside Drive
Aztec West
Almondsbury
Bristol BS32 4UD

Tel: 01454 624400 Fax: 01454 624409

Statement of use
This document provides information for DEFRA and Environment Agency Staff about consistent standards for flood defence and constitutes an R&D output from the Joint DEFRA / Environment Agency Flood and Coastal Defence R&D Programme.

Contract Statement

SUMMARY

Under their joint R&D programme for Flood and Coastal Defence, Defra/Environment Agency are funding a Targeted Programme of research aimed at obtaining better predictions of flood water levels. In order to achieve this, advances in knowledge and understanding made over the past three or four decades in the estimation of river conveyance will need to be introduced into engineering practice.

The project relates particularly to water level estimation, leading to a reduction in the uncertainty in the prediction of flood levels and hence in flood risk, and consequently facilitating better targeting of expenditure. The project will equally benefit the targeting of maintenance by providing better estimates of the effects of vegetation and its management. It is expected that the application of this knowledge from UK engineering research will have an international impact through improving the methods available to consultants.

The above objectives will be achieved through two core components of the new Conveyance Estimation System (CES) that will be developed: the Conveyance Generator and the Roughness Advisor. The CES is to be designed so that new knowledge from a parallel Strategic Programme of research can be integrated into the CES in due course.

This report is the designated output for Task T2 of the Targeted Programme of research. The Task objective is to review, select, code and test appropriate one-dimensional conveyance estimation methods for natural and engineered river and floodplain systems. The conveyance estimation methods will then be incorporated in the CES, comprising the Conveyance Generator component.

A review of the calculation methodology in the existing one-dimensional hydrodynamic modelling software ISIS, HECRAS and MIKE11 is provided. These are principally based on historic hand-calculation methods, with little or no account taken of the more recent advances in understanding and knowledge. The approaches include variations on the Divided Channel Method, which ignore the turbulence generated due to secondary flows and shearing, and tend to under and over-predict main channel and floodplain flows respectively.

A systematic review of alternative conveyance methods, starting from Knight's (2001) review is provided. Two key approaches are identified: (i) the energy loss approach and (ii) the depth-integrated Reynolds-Averaged Navier-Stokes approach, which have both been thoroughly assessed in terms of the physical basis, applicability for a range of channel types and ease of solution within the Conveyance Generator. The first approach (i), which divides the flow domain into sections representing different flow processes, is limited in that it can only be applied to trapezoidal channels, the calculated conveyance is reach-averaged rather than cross-sectional based and local friction values cannot be specified across the channel section. The second approach (ii) has been selected as it is physically based, it incorporates all the energy loss mechanisms present in a channel, it can be applied to any cross-section topography and has the added advantage of providing lateral velocity and bed shear stress profiles. This approach involves the calibration of four parameters; the local friction, the dimensionless eddy viscosity, the secondary flow term and the meandering coefficient.

The final calculation methodology is outlined in detail. The algorithms are solved numerically with the finite element method. The method has been tested against both physical models and real river measurements purpose made for research. For straight prismatic two-stage channels, the approach compares well to the observed flow conditions, including the bed shear stress predictions. For the skewed and meandering channel comparisons, the stage-discharge predictions accurately capture the trend of the data, and the depth-averaged velocity predictions follow the observed data reasonably well for most cases. A secondary flow model for the transition from straight to fully meandering channels has been proposed. Advice on the value for the meandering coefficient is provided, based on calibrated values for different sinuosities.

The Conveyance Generator stage-discharge predictions are compared to those of ISIS, and found to follow the trend of the data more accurately than the estimation based on historic approaches.

A sensitivity analysis is undertaken for the four calibration parameters and the dependence of conveyance on the reach-averaged longitudinal bedslope. The model has been found to be relatively insensitive to changes in calculation of the local friction, the dimensionless eddy viscosity and the secondary flow term. Estimation of the bedslope within ±100% of the actual value is found to provide the conveyance to within 3% of the actual value.

In general, the depth-integrated Reynolds-Averaged Navier-Stokes approach has been found to be a substantial improvement on the more historic, empirically based formulae. It has the added advantage of incorporating the lateral variations in local roughness, velocity and bed shear stress, as well as having a sound physical basis. It further satisfies the criteria outlined in the terms of reference,

“Develop selected method(s) to cover all cases of river/floodplain morphology. Ideally there should be a single unified method, with mechanism related terms which drop out or take zero values in various cases, determined by the measurable river system parameters mentioned above.”

CONTENTS

Tables

Figures

Appendices

SYMBOLS

Latin Alphabet

$A(x,t)$	cross-sectional area (m^2) (St Venant Equations)
A	flow area of sub-division (m^2) (HECRAS)
A_e	effective flow area (m^2) (MIKE11)
a_i	area of trapezium/triangle enclosed by points (x_i, y_i) and (x_{i+1}, y_{i+1}) on the bed and the water surface vertically above these points (m^2) (ISIS)
a	selected coefficient for open channel flow geometries Colebrook-White equation
B	water width at depth y (m) (MIKE11)
b	selected coefficient for open channel flow geometries Colebrook-White equation
C	Chezy coefficent ($m^{0.5}/s$)
C_l	energy loss coefficient (energy loss method)
C_{uv}	coefficient for sinuosity
c	selected coefficient for open channel flow geometries Colebrook-White equation
D_r	relative depth (m/m)
d	pipe diameter (m) Colebrook-White equation
E	total elements
Fr	Froude Number
f	local boundary friction factor based on the local substrate/vegetation roughness
f'	bedform roughness
g	gravitational acceleration (m/s^2)
H	local water depth normal to the bed (m)
H_{max}	maximum depth for a given channel section (m)
h	water level (m)
i	general element
i_b	bed slope (m/m)
K	cross-sectional channel conveyance (m^3/s)
k	secondary flow term coefficient
k	unit conveyance (= K/m) (m^2/s) (under program outputs)
k_s	absolute roughness height (m)
M	Manning number / Strickler coefficient ($m^{1/3}/s$)
M	linear operator (FEM)
N_p	number of cross-section points in panel p (ISIS)
N	number of parallel channels (MIKE11)
n_e	engineering 'n' which is all encompassing ($s/m^{1/3}$)
n_i	Manning's n defined at point (x_i, y_i) (ISIS) ($s/m^{1/3}$)
n_l	local 'n' includes local boundary friction losses only ($s/m^{1/3}$)
n	Manning's roughness coefficient ($s/m^{1/3}$)
$Q(x,t)$	discharge (m^3/s)v (St Venant Equations)
q	unit flow rate (m^2/s)
q_x	streamwise unit flow rate (m^2/s)
q_y	lateral unit flow rate (m^2/s)
q_n	unit flow for iteration n (FEM) (m^2/s)
Δq_n	incremental change in q_n (FEM) (m^2/s)
P	number of vertical panels (ISIS)
p	percentage (%)
$q(x,t)$	a lateral inflow for the discharges from small rivers (m^2/s)
R	hydraulic radius of sub-division (area / wetted perimeter) (m) (ISIS)

R	flow domain (FEM) (m^2)
R_*	resistance radius (Section 2.4 MIKE11)
R_h	hydraulic radius (m) (Section 2.4 MIKE11)
Re	Reynolds Number
R_m	hydraulic mean depth or ratio of area to surface width (m) (Section 5.2)
r_r	relative resistance (Section 2.4 MIKE11)
rpl_i	relative path length associated with panel p (ISIS)
S_f,	streamwise water surface/friction gradient
S_o	reach-averaged longitudinal bedslope
s	sinuosity (energy loss approach)
T	fluid temperature (°C)
t	time (s) (St Venant Equations)
U_d	depth-averaged streamwise velocity (m/s) (RANS approach)
U_*	shear velocity (m/s)
U_{ave}	average velocity (m/s)
u	streamwise velocity component at a given depth (m/s)
u_o	*critical velocity for incipient motion of that sediment size (m/s)*
u_1	velocity at which the Froude Number is 1.0 (m/s)
V_d	depth-averaged lateral velocity (m/s) (RANS approach)
v	lateral velocity component at a given depth (m/s)
v	velocity of the flow zone (m/s) (energy loss method)
wp_i	linear distance between (x_i, y_i) and (x_{i+1}, y_{i+1}) i.e. wetted perimeter (m) (ISIS)
x	streamwise direction parallel to the bed (m)
$\mathbf{x}$	vector of all contributing functions that are independent of Δq_n (FEM)
y	local water depth (m) (MIKE11)
y	lateral distance across section (m) (RANS approach)

Greek alphabet

α	Coriolis (or 'energy') coefficient
β_m	Boussinesq (or 'momentum) coefficient
β	coefficient for the influence of lateral bedslope on the bed shear stress (RANS approach)
Γ	secondary flow term for straight prismatic channels
Γ^*	scaled secondary flow term
Γ^*_{ave}	average scaled secondary flow term
ε	eddy viscosity (m/s^2)
λ	dimensionless eddy viscosity
λ_{mc}	main channel dimensionless eddy viscosity
ν	kinematic viscosity of the fluid (m^2/s)
σ	sinuosity - thalweg length over the valley length (m/m)
ρ	fluid density (kg/m^3)
τ_{ave}	laterally averaged boundary shear stress (N/m^2)
τ_b	bed shear stress (N/m^2)
τ_d	two-dimensional shear stress (N/m^2)
τ_{yx}	Reynolds stress (N/m^2)
ϕ	linear shape functions
χ	relaxation factor

ABBREVIATIONS

ADV	Acoustic Doppler Velocity
CES	Conveyance Estimation System
CG	Conveyance Generator
COHM	Coherence Method
DCM	Divided Channel Method
DEFRA	Department for Environment, Food and Rural Affairs
EA	Environment Agency
EBS	Ervine, Babaeyan-Koopaei and Sellin
EDM	Exchange Discharge Method
EPSRC	Engineering and Physical Sciences Research Council
FCF	Flood Channel Facility
FEM	Finite Element Method
HR	Hydraulic Research
LDM	Lateral Distribution Method
MDSF	Modelling and Decision Support Framework
RA	Roughness Advisor
RANS	Reynolds-Averaged Navier-Stokes
RHS	River Habitat Survey
SKM	Shiono & Knight Method
SP	Strategic Programme
TP	Targeted Programme
UE	Uncertainty Estimator
UK	United Kingdom
1D	One Dimensional
2D	Two Dimensional
3D	Three Dimensional

1. INTRODUCTION

1.1 Background

This report is a designated output for the Targeted Program (TP) of research being undertaken by HR Wallingford into reducing uncertainty in the prediction of flood levels. The principal aim of the work is improving the estimation of the discharge capacity of watercourses for the prediction of flood levels, velocities and the extent of the inundation. The end product will be a set of software tools, the Conveyance Estimation System (CES), to be adopted at a national scale. This CES will comprise three sub-components:

- Conveyance Generator CG (improved stage-conveyance calculation)
- Roughness Advisor RA (improved estimate of local resistance)
- Uncertainty Estimator UE (indication of uncertainty associated with CES outputs)

The CES will be available as open code, and can thus be incorporated into any one-dimensional hydrodynamic modelling package e.g. HECRAS, HYDRO-1D, ISIS, MIKE11 to improve the conveyance prediction for solution of the St Venant Equations. Alternatively, it can serve as a tool for further educational/academic research.

The TP includes nine technical tasks which have been identified together with a project management and integration component. Interim Report 2 documents Task T2, the development of the Conveyance Generator component of the CES. This task is intended to identify the methods for conveyance estimation that are most suitable for both inbank and out-of-bank flows. In short, this involves the review, selection, coding and testing of the appropriate one-dimensional conveyance estimation methods for natural and engineered river and floodplain systems. This report comprises the key deliverable of Task T2.

1.2 Terms of Reference / Objectives

The objectives of Task T2 of the Targeted Programme, as outlined in the Scoping Study (2001) specification include:

- Review and evaluate existing recent conveyance methods and select method(s) for development and testing. The selected method should be soundly based both physically and mathematically. Any empirical coefficients should be stable and predictable from readily measurable river parameters and specialist user interpretation should not be necessary.
- Develop selected method(s) to cover all cases of river/floodplain morphology. Ideally there should be a single unified method, with mechanism related terms which drop out or take zero values in various cases, determined by the measurable river system parameters mentioned above.
- Develop spreadsheet method in open code to implement method(s), and test/ develop iteratively against T-1 datasets. Behind the Conveyance Estimator will be a Conveyance Generator based on the preferred conveyance method, which will generate stage/conveyance tables. This will probably be written in Visual Basic in an Excel environment and for consistency must permit the same piece of code or at

least identical algorithms to be used in the code which will be included in the commercial one-dimensional models.

- Produce user spreadsheet, which will take unit roughness values from Task T5, which facilitates access to expert knowledge and information of UK rivers and floodplains, and thus produce stage-discharge curves and other outputs. This will form a sub-component of the overall CES.

During the development and implementation of Task T2, these original specifications were slightly altered, as the expert research panel, user consultative group and the project team agreed on appropriate improvements. The emphasis was changed from Microsoft Excel and the associated spreadsheet environment.

The TP includes a substantial action on providing a small set of recommended methods for conveyance estimation based on the plethora of methods identified in the Scoping Study review. The recommended methods will cover the full range of conditions which are likely to occur in British rivers under normal flow conditions to extreme floods.

1.3 Layout of this report

The remainder of this report is laid out as follows:

Section 2: A review of conveyance estimation methods currently incorporated in one-dimensional hydrodynamic models.

Section 3: A systematic evaluation of alternative conveyance methods that have been developed over the past two decades, starting with the review by Knight (2001), which forms part of the Annex to the Scoping Study (2001). A comparison of the two preferred conveyance estimation approaches.

Section 4: A thorough review of the selected method and its evolution, including the role of the various energy loss terms and empirical/calibration coefficients under different flow conditions.

Section 5: Description of the solution technique for the chosen method, including the finite element algorithm, details of the program structure and required input and output information. A brief review of the typical channel flow features that the CG will predict.

Section 6: Results and discussion of the testing of the conveyance method against a selection of laboratory flume data and purpose-made real river measurements. These tests incorporate stage-discharge predictions for a given channel cross-section geometry and resistance; as well as unit flow rate, depth-averaged velocity and bed shear stress distributions across these sections for a given depth of flow.

Section 7: Sensitivity tests for the calibration/empirical parameters and the role of the various terms in the equation. Comparison of the results with the cross-section conveyance predictions from the one-dimensional hydrodynamic modelling package, ISIS.

Section 8: Conclusions drawn from this initial testing of the selected conveyance approach, in view of the recognised method limitations.

Section 9: Recommendations for future research which may be incorporated within the timeframe for the Strategic Program SP.

Section 10: References.

2. CONVEYANCE ESTIMATION METHODS IN EXISTING RIVER MODELLING PACKAGES

2.1 One-, two- and three-dimensional modelling packages

One-dimensional hydrodynamic models are the most effective solution for the prediction of water levels, for a given discharge, in the foreseeable future. For clarity, the definitions of higher dimensional modelling used in this section (Scoping Study 2001) are:

- 2D models: solution of the 2D Shallow Water equations with an assumed velocity profile in the vertical direction, a hydrostatic pressure assumption and no calculation of vertical velocities.
- Layered models: solution of the 2D shallow water equations in a number of vertical layers (Falconer and Lin 1997). This allows the inclusion of some 3D effects, but usually still maintains the hydrostatic pressure assumptions.
- 3D models: solution of the complete momentum equation in all directions and incorporation of vertical acceleration and velocity. This approach requires a model for the position of the free surface.

The key issues for higher order modelling sighted in the Scoping Study (2001) are:

- the construction of higher order models is time-consuming and unnecessary as 1D models are usually the most appropriate technique. 2D and 3D models should rather be used where they may give better understanding than a standard 1D section and "cell" based approach
- the level of mesh refinement necessary for a finite element approach would be difficult to achieve with current computational resources and density.
- 2D models compromise between accuracy and stability when dealing with wetting and drying.
- in 2D models, depth-averaged velocity assumptions neglect vertical accelerations and secondary flow cells.
- a more accurate, but computationally expensive model is the layered model e.g. TELEMAC-3D (1997). This is suitable for wide water bodies where significant variations of velocity, temperature and salinity with depth are expected.
- 3D modelling of channel flow is predominantly still a research tool. As with 2D modelling, it should not be seen as a future alternative to 1D modelling, but rather as a complementary tool.

The primary outcome of the Scoping Study was that no actions on higher dimensional modelling are proposed in the Targeted Programme, but the Strategic Programme contains several potential topics to improve the technology and practice of 2D and 3D modelling.

The advantages of one-dimensional hydrodynamic models are that:

- they are easy to build from a series of representative channel cross-sections
- the computational time is short relative to higher dimensional models

- the computational space/storage requirement is less, thus enabling longer river reaches to be simulated
- less information is necessary e.g. local topography and roughness details
- setting up the model is less time consuming than higher order models

There are, however, some drawbacks as:

- they are less accurate in their representation of the physics of the flow
- the level of output detail is less (e.g. no lateral/vertical distributions of unit flow, velocity, bed shear stress, friction velocity etc)

For numerical simulation of the river dynamics, the classical hydraulic (vertically integrated) equations in the form of the Saint-Venant equations are used in these 1D models i.e. the mass conservation / continuity equation:

$$\frac{\partial Q}{\partial x} + \frac{\partial A}{\partial t} = 0 \tag{2.1}$$

(a change in level with time due to a change in flux) and the momentum conservation / dynamic equation:

$$\underbrace{\frac{\partial Q}{\partial t}}_{\text{(I)}} + \underbrace{\frac{\partial}{\partial x}\left[\frac{\beta Q^2}{A}\right]}_{\text{(II)}} + \underbrace{gA\left[\frac{\partial h}{\partial x} - S_o\right]}_{\text{(III)}} + \underbrace{g\frac{AQ|Q|}{K^2}}_{\text{(IV)}} = 0 \tag{2.2}$$

where:

$Q(x,t)$	=	discharge (m^3/s)
t	=	time (s)
x	=	streamwise direction (m)
$A(x,t)$	=	cross-sectional area (m^2)
g	=	gravitational acceleration (m/s^2)
h	=	water level (m)
S_o	=	bed slope (m/m)
K	=	conveyance (m^3/s)
β	=	Boussinesq coefficient

and

(I) local acceleration term
(II) convective term (responsible for non-linearity of equation)
(III) pressure term due to change in depth over reach – if S_o is neglected, then dh/dx approximates the friction slope based on the change in water level
(IV) source/gravity term causes water to flow

In some instances, equation 2.1 is set as equal to $q(x,t)$ m^2/s, which specifies a lateral inflow for the discharges from small rivers. Underground sources and ground waters can influence the lateral inflow and this directly influences the calculation.

The assumptions inherent in the application of equation 2.1 and 2.2 are that:

- the flow is one-dimensional i.e. a single velocity and elevation can be used to describe the state of the water body in a cross-section
- the water is incompressible with a constant density (=1000 kg/m^3) uniformly distributed
- the bed slope is small
- the streamline curvature is small and vertical accelerations are negligible, hence the pressure is hydrostatic
- the effects of boundary friction and turbulence can be accounted for by representations of channel conveyance derived for steady state flow
- all functions and variables are continuous and differentiable

Sections 2.2-2.4 comprise a summary and analysis of the conveyance estimation methods for determining '*K*' in equation 2.2, used in existing one-dimensional packages such as ISIS, HECRAS and MIKE11. This follows from Knight's (2001) suggestion that a thorough comparison of different methodologies used in commercial 1-D software for determining conveyance capacity of a channel would be most desirable, especially if related to errors in overbank conveyance.

Conveyance is defined as (Scoping Study, 2001) a quantitative measure of the discharge capacity of a watercourse. It relates total discharge to a measure of the 'energy' or 'friction' gradient S_f, through

$$K = \frac{Q}{S_f^{1/2}} \tag{2.3}$$

2.2 ISIS

The conveyance is calculated in ISIS by dividing the channel into a number of user defined vertical panels and summing the contribution from each panel. This divided panel approach is adopted to correct for the apparent reduction in conveyance as the water exceeds bankfull level. This unphysical phenomenon occurs in the single panel analysis, due to a significant increase in wetted perimeter within a small range of water levels. The cross-section conveyance is estimated from (ISIS V2.0, 2001):

$$K(h) = \sum_{p=1}^{P} \left[\left(\frac{\left(\sum_{i=1}^{N_p - 1} a_i \right)^5}{\left(\sum_{i=1}^{N_p - 1} wp_i \right)^2} \right)^{1/3} \frac{\left(\sum_{i=1}^{N_p - 1} wp_i \right)}{\left(\sum_{i=1}^{N_p - 1} n_i wp_i \right) \sqrt{rpl_p}} \right] \tag{2.4}$$

where:

a_i	=	area of trapezium/triangle enclosed by points (x_i, y_i) and (x_{i+1}, y_{i+1}) on the bed and the water surface vertically above these points (m^2)
wp_i	=	linear distance between (x_i, y_i) and (x_{i+1}, y_{i+1}) i.e. wetted perimeter (m)
n_i	=	Manning's n defined at point (x_i, y_i)
N_p	=	number of cross-section points in panel p
rpl_i	=	relative path length associated with panel p (some measure of panel sinuosity where zero sinuosity gives a rpl = 1.0)
P	=	number of vertical panels

These parameters are illustrated in Figure 2.1.

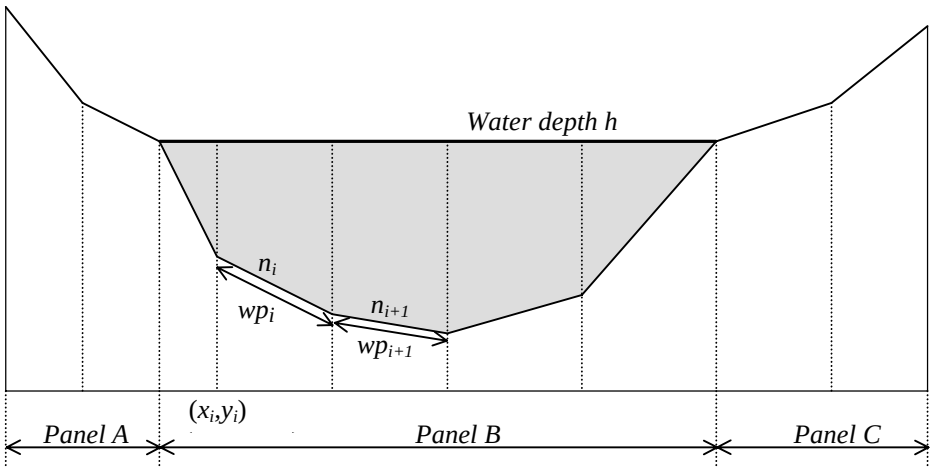

Figure 2.1 Definition sketch for the ISIS conveyance calculation

This formulation is based on the Divided Channel Method (DCM), which is essentially applying the Manning equation within separate "panels". This approach is limited as:

- it is empirically derived i.e. not based on rigorous physics
- it ignores the turbulence generated by the shear stresses between the vertical slices
- it ignores secondary currents thus over- and underestimating floodplain and main channel conveyance respectively
- the solution is dependent on the number of panels
- a single panel cannot have Manning's n values that differ by more than 20% and the ISIS guidelines do not recommend small panels. Thus roughness representation is difficult in sections of rapidly varying roughness.

In the case of dead floodplain storage (i.e. no conveyance) a zero Manning's n value is specified. The result is that the source/gravity term, term (IV) in equation (2.2), is approximately zero, due to division by the large conveyance value squared.

Knight (2001) found that when dealing with roughness there remains some uncertainty concerning the values for simple 1D parameters such as roughness and energy gradient. Usual calibration methods require the depth versus roughness relationship to be

determined. The method within ISIS is somewhat problematic due to assumptions inherent in how the roughness is distributed between nodal points.

2.3 HECRAS

The determination of total conveyance and the velocity coefficient for a cross-section requires that the flow be subdivided into units for which the velocity is uniformly distributed. The HECRAS (HECRAS, 1998) approach is thus to subdivide the flow in overbank areas using the input cross-section Manning *n*-value break points as the basis for this sub-division. The conveyance is calculated for each sub-division from:

$$K(h) = \frac{AR^{2/3}}{n} \tag{2.5}$$

where: n = Manning's roughness coefficient for sub-division
A = flow area of sub-division (m^2)
R = hydraulic radius of sub-division (area / wetted perimeter) (m)

The program sums the incremental conveyances in the overbank sections to obtain a total for the left and right overbank flow, while the main channel conveyance is computed as a single element. The total conveyance is obtained from summing these three contributions. Figure 2.2 illustrates this approach.

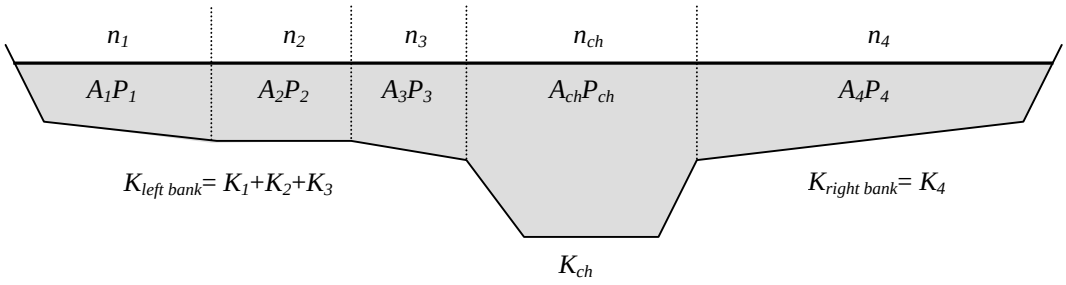

Figure 2.2 Definition sketch for the HECRAS conveyance calculation

An alternative method in HECRAS is to calculate conveyance between each co-ordinate point in the overbank region. This method will provide a different solution where sections on the floodplain have significant vertical slopes. In general, the default method provides a more conservative option for the same water surface elevation.

The flow in the main channel is only sub-divided if the roughness coefficient changes. HECRAS then tests the applicability of dividing the main channel, and if the main channel side slope is steeper than 0.2%, a single composite *n* value is computed from:

$$n_{mc} = \left[\frac{\sum_{i=1}^{N} \left(p_i n_i^{1.5} \right)}{P_{ch}} \right]^{2/3} \tag{2.6}$$

The HECRAS approach is essentially a DCM and is subject to similar limitations as expressed in Section 2.2 for ISIS.

2.4 MIKE11

MIKE11 (MIKE11, 1995) allows for two different descriptions of the bed resistance, both the Chezy and Manning coefficient. This simply alters the definition of term (IV) in equation 2.2 i.e.:

$$\frac{gQ|Q|}{C^2AR} \qquad \text{(Chezy coefficient)} \tag{2.7}$$

$$\frac{gQ|Q|}{M^2AR^{4/3}} \qquad \text{(Strickler formula)} \tag{2.8}$$

where M is the Manning number (=1/n) which is equivalent to the Strickler coefficient. The Chezy coefficient is related to Manning's n (Cunge *et al* 1980):

$$C = \frac{R^{1/6}}{n} = MR^{1/6} \tag{2.9}$$

The R in equation (2.7-2.9) is calculated using either a resistance radius R_* or a hydraulic radius R_h. The variation of resistance across a section is defined by a relative resistance, r_r. The effect of the r_r values on the hydraulic parameters in the processed data is dependent on whether R_* or R_h is used.

The hydraulic radius R_h formulation is based on a parallel channel analysis where the total conveyance of the section at a given elevation is equal to the sum of the conveyance of the parallel channels. These parallel channels are defined as those parts of the channel where the relative resistance, r_r, remains constant. If N is the number of parallel channels, the conveyance is given by,

$$K = \sum_{i=1}^{N} K_i = \sum_{i=1}^{N} \frac{A_i R_{hi}^{2/3}}{r_{ri} n} \tag{2.10}$$

and for a given total channel cross-sectional area A,

$$R_h = \left[\frac{\sum_{i=1}^{N} \left(\frac{A_i^{5/3}}{r_{ri} P_i^{2/3}} \right)}{A} \right]^{3/2} \tag{2.11}$$

The resistance radius R_* is given by (Engelund 1966),

$$\sqrt{R_*} = \frac{1}{A}\int_0^B y^{3/2}\,db \tag{2.12}$$

where: y = *local water depth (m)*
B = water width at depth y (m)

This formulation ensures that the Manning number M is almost independent of the water depth (MIKE11, 1995) in the case of composite cross sections. It further relates the velocity to the depth, in a similar manner to the Chezy equation however it neglects the lateral stresses. The relative resistance r_r is included in this formulation by adjusting the physical flow area to give the effective flow area A_e (m^2) as,

$$A_e = \sum_{i=1}^{N}\left(\frac{A_i}{r_{ri}}\right) \tag{2.13}$$

where: N = number of sub-sections which equals the number survey data points less one

One disadvantage is that R_h does not have a simple geometric interpretation when $r_r \neq 1.0$ and similarly A_e is not a physically measurable area for $r_r \neq 1.0$. Both are calculation devices, which are defined to give a realistic value of conveyance, however, they are open to incorrect interpretation by the casual user e.g. less-skilled users may assume the effective area is the actual area.

Comparison of the R_h and the R_* approach yield the following conclusions:

- R_* allows a smooth transition in conveyance as the bankfull depth is exceeded.
- In the deeper sections, the R_h option is more conservative, as the R_* overestimates conveyance in deep, narrow cross-sections as it does not account for the friction at the cross-section sides.
- R_* more is suitable for cross-sections with significant changes in shape e.g overbank flow paths.
- The analysis of wide channels will yield similar results for R_h and R_*.

Both of the approaches incorporated in MIKE11 are essentially based on a modified form of the DCM and are subject to the limitations outlined in Section 2.2.

3. CONVEYANCE ESTIMATION METHODS; RESEARCH AND REVIEW PROCESS

This section outlines the conveyance estimation review process, from Knight's (2001) expert paper on method development over the past two decades through to more recent work that has been undertaken. Two preferred approaches are identified and assessed in view of the criteria outlined in the terms of reference (Section 1.2), in particular, the mathematical and physical basis of the model and its applicability to a range of channel conditions.

3.1 Advances in conveyance estimation

Historically, conveyance predictions were based on simple hand calculation methods. A single discharge for a whole channel cross-section was computed, and the different approaches varied in their approximation of a composite roughness or Manning's '*n*' value. Methods typically include those of Pavlovskii (1931), Lotter (1933), Horton & Einstein (1933-34), Einstein & Banks (1950) and Krishnamurthy & Christensen (1972).

Research over the past twenty years, including a managed programme of research on the EPSRC Flood Channel Facility (FCF) at HR Wallingford, reflects a vast improvement in the calculation approach to channel conveyance. This ranges from the understanding and interpretation of the complex flow mechanisms in a channel section, to the advent of computing tools that enable more sophisticated solution techniques. An extensive and ever-increasing database of both physical model and real river measurements has provided a sound basis for testing these research advances. Significant contributions include those of Chang (1983), Ervine & Ellis (1987), Shiono & Knight (1989), Ackers (1991-93), James & Wark (1992), Ervine *et al* (2000) and Bousmar & Zech (2002).

Knight's expert paper identified various methods for estimating conveyance, providing a thorough assessment of any limitations in the physics or implementation of these approaches. This included assumptions in the derivations such as quasi-straight channel reaches and negligible lateral momentum transfer for the early DCMs that many 1D river modelling packages are based on (Section 2).

The Scoping Study (2001) drew out some of the key messages from Knight's paper:

- The improved DCM methods may perform well in given circumstances, however, they are not based on rigorous physics and cannot be broadly accepted.
- The coherence method (COHM) of Ackers requires an idealised trapezium section and is therefore not readily applicable to natural channels.
- The lateral distribution method (LDM) ignores the secondary flow terms and simplifies the diffusion process through the use of a single 'catch-all' parameter.
- The Shiono & Knight method (SKM) extends the physical basis of the LDM method, and despite the difficulty of estimating the three calibration coefficients, the physical basis of this method provides much promise, albeit for straight prismatic channels only.

Furthermore, Knight's expert paper makes the distinction between 'global', 'zonal' and 'local' roughness coefficients which refer to the whole cross-section, the sub-area of a

cross-section or the 'unit strip' of boundary respectively. These concepts are essential to the scale at which the conveyance is calculated and are thus revisited in Section 4 for the selected approach.

The Exchange Discharge Model (EDM) (Bousmar & Zech; 2002) is a more recent one-dimensional approach for quantifying the momentum transfer between the main channel and prismatic or non-prismatic floodplains. Two physical concepts, (i) turbulent exchange due to shear layer development and (ii) geometrical transfer due to cross-sectional changes, are identified and quantified as proportional to the velocity gradient at the interfaces of the channel sub-sections. While an improvement on the earlier DCMs, this approach provides similar results to the LDM for natural rivers, and it requires calibration of both the turbulent and geometrical exchange parameters.

Both the straight channel methods reviewed in Knight's expert paper and the more recent EDM are not applicable to the meandering channels found in nature. Meandering channels are more complex as the associated loss mechanisms include the effects of helical secondary currents, increased turbulence, expansion and contraction (flow between the main channel and floodplain) and variations in cross-stream water levels. The combination and level of influence of the different loss mechanisms is further dependent on the sinuosity, relative depth and the ratio of floodplain to main channel roughness (Ervine *et al*, 2000). Previous research on meandering channels has focused on inbank flow, thus eliminating difficulties associated with the change in the predominant velocity direction from within the main channel to out-of-bank and floodplain flow. More recently, research has extended to two-stage meandering channels. Two key approaches have been identified:

(i) **The Energy Loss Approach:** Division of channel cross-section into physically identifiable units, representing different flow mechanisms, and hence summing the energy loss contributions (Ervine & Ellis, 1987; Shiono *et al*, 1999).

(ii) **The RANS Approach:** Depth-integration of the Reynolds Averaged Navier-Stokes (RANS) equations for flow in the streamwise direction (Shiono & Knight, 1990; James & Wark, 1992; Ervine *et al*, 2001).

These two approaches have been reviewed in terms of:

- the theoretical and physical basis of the method
- consideration of all energy losses
- representation of energy loss hierarchy with variation in water level/sinuosity e.g. change in secondary current direction and structure
- previous testing of method against physical model and real river data
- reliable and readily available calibration/empirical parameters
- the ease of method implementation for a range of channel types
- the outputs i.e.: discharge for a given water level (high priority)
  lateral velocity/bed shear stress distributions
- the nature and number of roughness coefficients
- reach or cross-section analysis

3.2 Energy loss approach

3.2.1 Method description

This approach is essentially a channel division method whereby the various energy loss mechanisms are identified within three flow zones; (i) main channel inbank flow, (ii) out-of-bank flow within the meander belt and (iii) floodplain flow outwith the meander belt (fig 3.1).

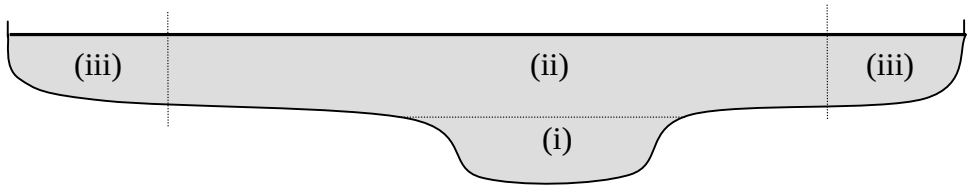

Figure 3.1 Channel sub-division into representative flow zones

The underlying assumption is that the energy loss contributions from the mechanisms within each flow zone are proportional to the square of the local flow velocity. For a given flow zone, with *n* energy loss types, the equation form is

$$\sum_{i=1}^{n} C_{li} \frac{v^2}{2g} = \frac{S_o}{s} \tag{3.1}$$

where:
- v = velocity of the flow zone (m/s)
- S_o = bedslope
- g = gravitational acceleration (m/s^2)
- s = sinuosity
- C_l = energy loss coefficient

The coefficient C_l assumes different values according to the energy loss it represents. The losses in the inbank region include boundary friction, secondary flows and streamwise turbulent shear stresses. Zone (ii) incorporates losses due to boundary friction, expansion and contraction of the flow and turbulent shear forces over the meander wavelength, while zone (iii) only includes boundary friction.

3.2.2 Method assessment

The energy loss approach has been evaluated (Table 3.1) in terms of the criteria set out in Section 3.1.

Table 3.1 Energy loss method evaluation

Criteria	Comment	Rating
Physical basis	The energy loss approach is based in physics. It considers the various flow zones and mechanisms in terms of the square of the local flow velocity, which is a widely used energy loss expression e.g. expansion and contraction losses in channel/pipe flow. However, the method does assume the principle of superposition.	7
Energy losses	It accounts for all the main energy loss mechanisms including those due to secondary flows and turbulent shear stresses on the zone interfaces, which are ignored in the earlier DCMs.	7
Energy loss hierarchy	The energy loss coefficient C_l varies with relative depth and sinuosity, however, it has only been tested against three different sinuosities, which are all less than 1.6.	5
Testing against lab & river data	Previous testing (Ervine & Ellis, 1987; Shiono *et al*, 1999) only includes experimental measurements (Toebes & Sooky, 1967, U.S. Corps. of Engineers, 1956; Muto, 1997; Muto *et al*, 1998; Shiono & Muto, 1998).	3
Reliable/available coefficients	The loss coefficients are derived from laboratory data. The suitability of these coefficients for real river data, with possible scale effects, has not been tested.	3
Ease of implementation for a range of channel types	The method is easy to understand and apply for an idealised section. It has not, however, been extended to handle irregular channel geometries and/or meander patterns.	1
Outputs	This method provides a stage-discharge curve and average velocities for the various flow zones.	7
Nature/number of roughness coefficients	The bed friction factor is determined from Darcy-Weisbach formula and a factor is determined for each flow zone. This limits the representation of localised bed features such as trees, boulders or change in crop type within a flow zone.	3
Reach or cross-section application	The losses are determined over a meander reach. This method would require conversion to a cross-sectional reference framework for implementation in 1D hydrodynamic models.	3
Other	The method is easy to understand as it describes each energy loss independently.	10

Key: 1= *worst* to 10 = *best* (Total : 49)

3.3 Reynolds-averaged Navier-Stokes (RANS) approach

3.3.1 Method description

This approach is based on the depth-integration of the RANS equations for flow in the streamwise direction. The basic form of the depth-averaged momentum equation for application to channel flow is (Shiono & Knight,1988):

$$\underbrace{\rho g H \frac{dh}{dx}}_{\text{(I)}} - \underbrace{\beta \tau_b}_{\text{(II)}} + \underbrace{\frac{\partial}{\partial y}\left(H\overline{\tau_{yx}}\right)}_{\text{(III)}} = \underbrace{\frac{\partial}{\partial y}\left[H\left(\rho\,\overline{UV}\right)_d\right]}_{\text{(IV)}} \qquad (3.2)$$

where:

ρ	= fluid density (kg/m^3)
g	= gravitational acceleration (m/s^2)
H	= local water depth normal to the bed (m)
h	= water level (m)
x	= streamwise direction parallel to the bed (m)
y	= lateral distance across section (m)
U_d	= depth-averaged streamwise velocity (m/s)
V_d	= depth-averaged lateral velocity (m/s)
τ_b	= bed shear stress (N/m^2)
τ_{yx}	= Reynolds stress (N/m^2)
β	= coefficient for the influence of lateral bedslope on the bed shear stress

and the terms represent the:

(I) variation in hydrostatic pressure along the reach
(II) boundary friction effects
(III) turbulence due to shearing between the lateral layers
(IV) turbulence due to secondary currents

The bed shear stress can be expressed in terms of the shear velocity U_* (m/s) and hence the depth-averaged velocity and bed friction factor f as,

$$\tau_b = \rho U_*^2 = \rho \frac{f}{8} U_d^2 \qquad (3.3)$$

The Reynolds' stress can be depth-averaged and expressed in terms of the eddy viscosity ε (m/s^2) as,

$$\overline{\tau_{yx}} = \frac{1}{H}\int_0^H \tau_{yx}\,dz = \rho\varepsilon\,\frac{\partial U_d}{\partial y} \qquad (3.4)$$

Substituting equations (3.3) and (3.4) into (3.2), approximating the friction slope with the longitudinal bedslope, S_o, and implementing the eddy viscosity model,

$$\varepsilon = \lambda U_* H \qquad (3.5)$$

where the depth 'H' is some measure of the turbulence length scale and λ is the dimensionless eddy viscosity which accounts for the viscosity variation with depth, yields the SKM (Shiono & Knight, 1990),

$$\rho g H S_o - \frac{\rho f \beta U_d^2}{8} + \frac{\partial}{\partial y}\left[\rho \lambda H^2 \left(\frac{f}{8}\right)^{1/2} U_d \frac{\partial U_d}{\partial y}\right] = \frac{\partial}{\partial y}\left[H\left(\rho \overline{UV}\right)_d\right] \tag{3.6}$$

Equation (3.6) can be solved analytically by dividing the cross-section into sub areas with specified boundary conditions. Alternatively, a numerical solution can be implemented whereby the channel cross-section is discretised (fig 3.2) into a number of flow elements, and finite difference/element approximations are substituted into the equation. The resulting system of equations is solved to find the local depth-averaged velocity within each element. The velocity distribution can thus be integrated to provide the total channel discharge.

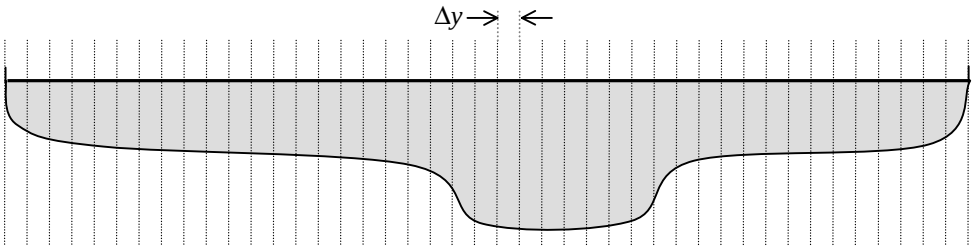

Figure 3.2 Channel discretisation for solution of depth-integrated RANS

However, a further difficulty is the unknown depth-averaged lateral velocity distribution V_d. Previously, two approaches have been examined:

(i) *Straight prismatic channels*

The SKM (Shiono & Knight, 1990) implements a secondary flow term, Γ ($= \rho\left(\overline{UV}\right)_d$), which is a calibration coefficient that varies laterally across the channel. It assumes different values for main channel and floodplain flows, and the value increases with increased relative depth, as the nature/direction of the secondary currents change.

(ii) *Meandering channels*

The EBS method (Ervine *et al*, 2000) extends the SKM method to incorporate the secondary flow effects resulting from meandering channels. A coefficient C_{uv}, which relates the secondary currents to the depth mean velocity, is introduced such that,

$$\overline{UV} = C_{uv} U_d^2 \tag{3.7}$$

where C_{uv} attains a single value for a given cross-section and it is a function of the sinuosity, relative depth and relative roughness. The assumption is that the product of the local U and V velocities averaged over the depth, follow a similar profile to the streamwise depth-averaged velocity squared.

3.3.2 Method assessment

The RANS approach has been evaluated (Table 3.2) in terms of the criteria set out in Section 3.1.

Table 3.2 RANS method evaluation

Criteria	Comment	Rating
Physical basis	The RANS approach is physically based as it is derived from the original Navier-Stokes equations for fluid flow. It should, however, be implemented with caution at high sinuosties, as the predominant velocity vector may change direction at bankfull.	7
Energy losses	It accounts for all the energy losses including bed friction, turbulence generated by secondary flows and turbulence due to shearing between the vertical layers.	7
Energy loss hierarchy	The change in energy losses due to increased sinuosity and relative depth is reflected in the loss coefficients: f, λ, Γ and C_{uv}.	7
Testing against lab & river data	Previous testing against both experimental and field measurements has been undertaken for SKM and EBS approach (Shiono & Knight, 1990; Ervine *et al*, 2000). The EBS approach was tested at the apex of the meander bend.	7
Reliable/available coefficients	The coefficients λ and Γ have previously defined relationships derived from laboratory data. Predictions have been compared to river data with reasonable results. The parameter C_{uv} has been used for both experimental and field cases, however, while the value is in the range 0-5% (straight to fully meandering channels), no clear guidance exists. Finding the balance of the four calibration coefficients to cover all possible flow cases provides a substantial challenge.	1
Ease of implementation for a range of channel types	This method can be applied to irregular river cross-sections and planform geometries. Although an analytical or numerical solution is required, the implementation is feasible in computer code, without requiring detailed knowledge by the user.	7
Outputs	This method provides the basic stage-discharge curve and has the added advantage of providing lateral depth-averaged velocity and bed shear stress distributions. These are useful for weed cutting and sediment transport predictions.	10
Nature/number of roughness coefficients	The bed friction factor can be derived from a standard formula e.g. Colebrook-White, Blasius or alernatively a local 'f' value can be provided thus enabling representation of localised bed features such as trees, boulders or artificial lining.	7
Reach or cross-section application	The method is applied to a cross-section and thus facilitates implementation for 1D hydrodynamic models.	7
Other	The method is difficult for the casual user to understand in detail.	3

Key: 1= *worst* to 10 = *best* (Total : 63)

3.4 Conclusion

Based on the assessment of the energy loss and RANS approach to estimating conveyance, the RANS approach has compared more favourably (scored 63 compared to 49). The project technical directors approved this approach and the academic advisory board has further supported it. In short, the RANS approach is: applicable to all channel types; is a cross-section based calculation; and, has a sound physical basis. It does, however, require the calibration of four coefficients and it should be applied to highly sinuous channels with caution. It is recognised that while no existing method is without fault, it is the intention of this project to provide an improvement for the current conveyance estimation methods employed in 1D hydrodynamic models. Thus provided all assumptions are clearly stated, the RANS approach should provide a substantial advance in current application and knowledge.

4. DEVELOPMENT OF THE RANS APPROACH

4.1 Derivation and unit flow rate

Based on the research and review process outlined in Section 3, the RANS approach to the conveyance estimation was selected for implementation in the CES. Equation (3.6) was derived from first principles to verify this approach and highlight any assumptions in the derivation (Appendix 1).

$$\rho\, gHS_o - \frac{\rho\, f\beta U_d^2}{8} + \frac{\partial}{\partial y}\left[\rho\,\lambda\, H^2\left(\frac{f}{8}\right)^{1/2} U_d\,\frac{\partial U_d}{\partial y}\right] = \frac{\partial}{\partial y}\left[H\left(\rho\,\overline{UV}\right)_d\right] \tag{3.6}$$

Previous research (Samuels, 1989) has advocated the solution of the unit flow rate, q (m^2/s), over the depth-averaged velocity U_d, due to the strong continuity properties of q with variations in depth e.g. across a vertical face/step in an engineered channel cross-section. The streamwise q_x and lateral q_y unit flow rates are defined as,

$$q_x = \int_0^H u\, dz = HU_d \qquad \text{and} \qquad q_y = \int_0^H v\, dz = HV_d \tag{4.1a,b}$$

where u and v (m/s) are the streamwise and lateral velocity components at a given depth. Assuming that the fluid density is constant throughout the section, and substituting q_x into equation (3.6) yields,

$$gHS_o - \frac{f\beta\, q_x^2}{8H^2} + \frac{\partial}{\partial y}\left[\lambda\, H\left(\frac{f}{8}\right)^{1/2} q_x\,\frac{\partial}{\partial y}\left(\frac{q_x}{H}\right)\right] = \frac{\partial}{\partial y}\left[\frac{\left(\overline{q_x q_y}\right)_d}{H}\right] \tag{4.2}$$

The derivation (Appendix 1) of the SKM/LDM methods, in terms of the unit flow, reveals that the LDM method (James & Wark, 1992) is subtly different from the SKM method (Shiono & Knight, 1990) in that it is only applicable to channels of constant depth. This is apparent in the third term of equation (4.2), where the depth H within the lateral differential term is cancelled with the H outside this term i.e.

LDM:
$$\frac{\partial}{\partial y}\left(\lambda\, q_x\left(\frac{f}{8}\right)^{0.5}\frac{\partial}{\partial y}(q_x)\right) \tag{4.3}$$

SKM:
$$\frac{\partial}{\partial y}\left(\lambda\, q_x \boldsymbol{H}\left(\frac{f}{8}\right)^{0.5}\frac{\partial}{\partial y}\left(\frac{q_x}{\boldsymbol{H}}\right)\right) \tag{4.4}$$

The result is that the depth-averaged velocity distribution (e.g. FCF Series 2 & 3, River Trent, River Main, River Penk etc in James & Wark, 1992) contains 'spikes' at laterally

varying gradients e.g. main channel side slopes. This third term is thus expressed in accordance with equation (4.4) throughout.

4.2 Sinuosity and the Secondary Flow Term

Equation (4.2) can be expressed for straight prismatic channels (Shiono & Knight, 1990) as,

$$gHS_o - \frac{f\beta q_x^2}{8H^2} + \frac{\partial}{\partial y}\left[\lambda H\left(\frac{f}{8}\right)^{1/2} q_x \frac{\partial}{\partial y}\left(\frac{q_x}{H}\right)\right] = \Gamma \tag{4.5}$$

and for channels of sinuosity greater than 1.1 (Knight DW & Ervine A, personal communication), as

$$gHS_o - \frac{f\beta q_x^2}{8H^2} + \frac{\partial}{\partial y}\left[\lambda H\left(\frac{f}{8}\right)^{1/2} q_x \frac{\partial}{\partial y}\left(\frac{q_x}{H}\right)\right] = C_{uv}\frac{\partial}{\partial y}\left[\frac{q_x^2}{H}\right] \tag{4.6}$$

where the sinuosity, σ, is defined as the thalweg length over the valley length. To obtain a balance between σ = 1.0 (equation 4.5) and σ > 1.1 (equation 4.6), the contribution from the Γ term is linearly phased out (Figure 4.1).

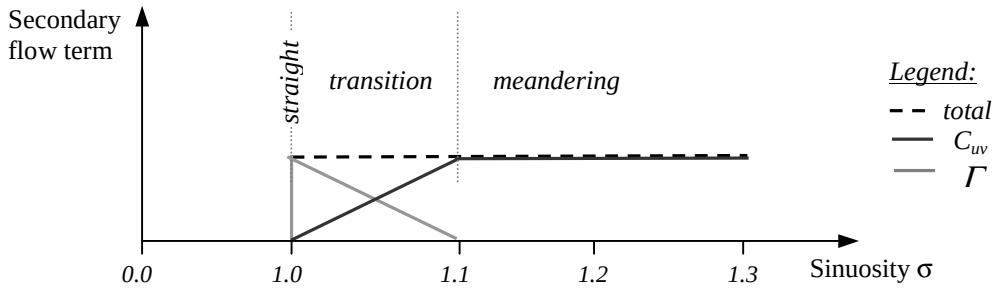

Figure 4.1 Contributions from the secondary flow terms

resulting in:

$$-\frac{(1.1-\sigma)}{0.1}\Gamma - \frac{(\sigma-1.0)}{0.1}C_{uv}\frac{\partial}{\partial y}\left(\frac{q_x^2}{H}\right) = 0 \qquad 1.0 \le \sigma \le 1.1$$

$$-C_{uv}\frac{\partial}{\partial y}\left(\frac{q_x^2}{H}\right) = 0 \qquad \sigma > 1.1 \tag{4.7a,b}$$

The continuity of the total secondary flow function should be verified, due to the assumption of adding the weighted contributions e.g. through the estimation of conveyance for a uniform section with increasing sinuosity.

4.3 Conveyance Generator equations

The final equations to be solved for in the Conveyance Generator (CG) are thus,

$$gHS_o - \frac{f\beta q^2}{8H^2} + \frac{\partial}{\partial y}\left[\lambda H\left(\frac{f}{8}\right)^{1/2} q \frac{\partial}{\partial y}\left(\frac{q}{H}\right)\right] = \frac{(1.1-\sigma)}{0.1}\Gamma + \frac{(\sigma-1.0)}{0.1} C_{uv} \frac{\partial}{\partial y}\left[\frac{q^2}{H}\right} \qquad 1.0 \le \sigma \le 1.1$$

$$gHS_o - \frac{f\beta q^2}{8H^2} + \frac{\partial}{\partial y}\left[\lambda H\left(\frac{f}{8}\right)^{1/2} q \frac{\partial}{\partial y}\left(\frac{q}{H}\right)\right] = C_{uv} \frac{\partial}{\partial y}\left[\frac{q^2}{H}\right] \qquad \sigma > 1.1$$

(4.8a,b)

and unless otherwise specified, the unit flow rate 'q_x' is referred to as 'q' for the remainder of this report.

4.4 Methodology and Evaluation of the terms in the CG Equations

The parameterisation and evaluation of each term in the final equation set (equations 4.8a,b) and its coefficients is discussed in this section. The unit flow rate, q, is the unknown parameter which the Conveyance Generator is initially solving for. Integration of the unit flow distribution provides the total channel discharge, Q, for a given stage. The conveyance, K, is given by equation (2.3),

$$K = \frac{Q}{S_f^{1/2}}$$

(2.3)

where the friction slope S_f is approximated by the bedslope S_o.

4.4.1 Source/hydrostatic pressure term

The source term, gHS_o, is evaluated from the gravitational acceleration g = 9.807m/s^2, the local cross-section water depth H (m) and an approximation to the friction slope based on the longitudinal bedslope, S_o. The implicit assumption is that the bedslope is approximately parallel to the water surface slope or friction slope, for the reach under study.

4.4.2 Boundary friction term

The boundary friction term,

$$-\frac{\beta f q^2}{8H^2}$$

together with the source term, comprises the primary balance of momentum in equation 4.8. Simplification of these two terms results in the well-known Darcy-Weisbach friction formulae. The coefficient β accounts for the influence of the transverse bedslope on the bed shear stress, and is evaluated from

$$\beta = \left(1 + S_y^2\right)^{1/2} \tag{4.9}$$

where S_y is the transverse bedslope. f is the local boundary friction factor based on the substrate/vegetation roughness. The lateral distribution of f is based on a form of the Colebrook-White (1937) equation,

$$\frac{1}{\sqrt{f}} = -2.0\log\left[\frac{k_s}{3.71d} + \frac{2.51}{\mathrm{Re}\sqrt{f}}\right](Colebrook-White: pipes)$$

$$\frac{1}{\sqrt{f}} = -\mathbf{c}\log\left[\frac{k_s}{\mathbf{a}H} + \frac{\mathbf{b}q}{4\nu\sqrt{f}}\right](open\ channel\ flow) \tag{4.10}$$

where:
k_s = absolute roughness height (m)
Re = Reynolds Number
ν = kinematic viscosity (m^2/s)
d = pipe diameter (m) which is equivalent to $4.0H$

and **a**, **b** and **c** are selected coefficients for open channel flow geometries. Based on previous research advice (Table 4.1), these coefficients for both engineered and natural channels are provided in Table 4.2. These values were obtained from averaging the coefficients for similar channel types, ignoring any outliers.

Table 4.1 Summary of previous 'Colebrook-White' coefficients for open channel flow

Researcher	c	a	b	Description
Zegzhda (1938)	2.00	11.55	-	Rectangular with dense sand
Keulegan (1938)	2.03	12.27	3.41	Wide & smooth flow channel
Keulegan (1938)	2.00	12.62	2.98	Wide & fully rough channel
Keulegan (1938)	2.03	12.27	3.09	Smooth trapezoidal channel
Keulegan (1938)	2.00	13.99	2.27	Rough trapezoidal channel
Rouse (1946)	2.03	10.95	1.70	Wide channels
Thijsse (1949)	2.03	12.20	3.03	Wide channels
Sayre & Albertson (1961)	2.14	8.89	7.17	Wide channels
Reinius (1961)	2.00	12.40	3.40	Wide channels
Henderson (1966)	2.00	12.00	2.50	Wide channels
Graf (1971)	2.00	12.90	2.77	Wide channels

Table 4.2 Coefficient values to be implemented in the Colebrook-White Equation

Application	c	a	b	Description
Laboratory/engineered	2.03	12.27	3.09	Smooth trapezoidal channel
Laboratory/engineered	2.00	13.99	2.27	Rough trapezoidal channel
Natural channels	2.01	12.40	3.02	Wide channels (smooth/rough)

The widely used Manning's *n*-value (Chow, 1959) is defined as an engineering 'n_e', as it incorporates the losses due to local friction, secondary flows, sinuosity, change in form, lateral shear stresses and channel irregularities. This engineering n_e is thus all encompassing. In addition, a local 'n_l' value is defined, which represents the local boundary friction losses due to substrate, vegetation and artificial substances only. As the parameters λ, Γ and C_{uv} account for the losses due to shearing, secondary flows and sinuosity respectively, the bed friction value *f*, determined from '*n*', need only describe the local energy losses.

The Roughness Advisor, which is a part of the CES based on the familiar concept of Manning's roughness, will provide the Conveyance Generator with this pure/local n_l value, based on the substrate and/or vegetation type. The Colebrook-White equation was selected in preference to the Manning equation, as (i) it covers smooth, transitional and rough flow conditions; (ii) it has a strong physical basis as it is derived from the logarithmic velocity profile together with the channel geometry and (iii) it incorporates the roughness variation with depth. The equivalent k_s value is determined from (Ackers, 1958),

$$n_l = 0.038 k_s^{1/6} \tag{4.11}$$

where the depth *H* is in the range of 7-140 times the magnitude of k_s. Although the roughness height, k_s, is traditionally defined in terms of the sand grain dimension (Nikuradse, 1933), the vegetation k_s-value can be interpreted as an equivalent length scale. Solution of equation (4.10), requires the kinematic viscosity ν (m^2/s) of the fluid. This can be determined from (Raudkivi, 1998),

$$\nu = (1.741 - 0.0499T + 0.00066T^2) \times 10^{-6} \tag{4.12}$$

where *T* (℃) is the fluid temperature.

Expert advice (Personal communication, Knight DW) is that the explicit solution of the Barr equation (1975),

$$\frac{1}{\sqrt{f}} = -2\log\left[\frac{k_s}{14.8D} + \frac{5.1286}{\mathrm{Re}^{0.89}}\right] \tag{4.13}$$

may be a suitable alternative to equation (4.10), should this iterative approach prove computationally expensive with respect to time. This will only become apparent in the final implementation of the CES in a one-dimensional hydrodynamic model.

The roughness height in alluvial channels varies as the velocity is increased. This typically occurs in tidal regions. The bed is smooth initially. As the velocity increases, ripples start to form, and as the velocity increases further, these develop into dunes. As the bedfoms grow, the bed resistance increases, and the transition from lower regime conditions to upper regime conditions is initiated. Flow along the bed becomes fully turbulent, the bedforms are broken down and fully turbulent conditions prevail within

the boundary layer. A further increase in velocity results in the development of upper flow regime bedforms e.g. antidunes.

A simple step-function (Figure 4.2) is introduced to approximate the bedform friction losses, where f is the roughness without bedforms, f' is the bedform roughness which can be calibrated as 2-4 times the magnitude of f, u_o is the critical velocity for incipient motion of that sediment size (Shields, 1936) and u_1 is the velocity at which the Froude Number is 1.0 (unlikely to occur).

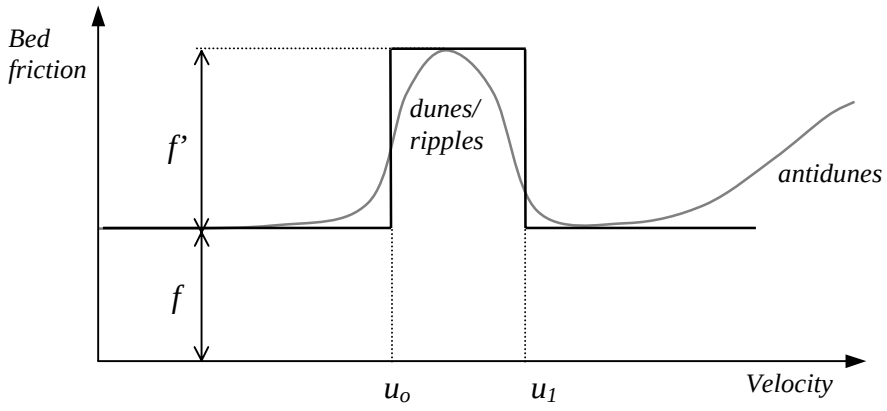

Figure 4.2 Step-function representation of bedform losses in an alluvial channel

4.4.3 Turbulence term for lateral shear

The turbulence generated through lateral shear between the vertical slices is given by,

$$\frac{\partial}{\partial y}\left[\lambda H\left(\frac{f}{8}\right)^{1/2} q \frac{\partial}{\partial y}\left(\frac{q}{H}\right)\right] \tag{4.15}$$

This term has a relatively small impact on the total discharge Q (m^3/s); however, it improves the lateral depth-averaged velocity and unit flow distributions.

Early research (Knight & Shiono, 1990; Knight & Shiono 1991; James & Wark, 1992) for calibrating the dimensionless eddy viscosity λ, has indicated typical values in the range 0.07 (experimental facilities) to 0.5 (natural channels). In general, λ is largest in the regions adjacent to the main channel – floodplain interface, where the turbulent eddies are generated. More recently the relative depth, D_r, and the main channel eddy viscosity, λ_{mc}, have been identified as appropriate means of describing the lateral distribution of λ (Abril, 2001), where

$$\lambda = \lambda_{mc}\left(-0.2 + 1.2D_r^{-1.44}\right) \tag{4.16}$$

and 0.07 (experimental) < λ_{mc} < 0.5 (real rivers). The value λ_{mc} = 0.24 has been employed in the Conveyance Generator, where the main channel is defined as within

the user assigned top of bank markers. The relative depth is defined as (Knight DW & Abril B, personal communication),

$$D_r = \frac{H}{H_{max}} \tag{4.17}$$

where H_{max} (m) is the maximum depth for a given channel section. The extreme values of D_r in equation (4.15) indicate that as $D_r \rightarrow 0$; $\lambda \rightarrow \infty$ and that the relative depth will always be less than or equal to 1.0.

4.4.4 Secondary flow term for straight channels

For straight channels, the sinuosity is 1.0, and thus the secondary flow term is given by,

$$\frac{(1.1-\sigma)}{0.1}\Gamma = \frac{(1.1-1.0)}{0.1}\Gamma = \Gamma \tag{4.18}$$

Research to date involves calibrating Γ for channels with known velocity distributions. This parameter is thus, ill-defined, despite being identified (Knight DW, personal communication) together with the friction factor '*f*', as being critical to the solution of equations (4.8a,b).

The scaled secondary flow term Γ^* is defined as (Abril, 2001),

$$\Gamma^* = \frac{\Gamma}{H} = \frac{\partial(\rho\overline{UV})_d}{\partial y} = \left(= \frac{1}{H}\frac{\partial}{\partial y}\left(\frac{\left(\rho\overline{q_x q_y}\right)_d}{H} \right) \right) \tag{4.19}$$

which is different to Γ by a factor of the local depth *H*. As the laterally averaged boundary shear stress, τ_{ave}, and the two-dimensional shear stress, τ_d (= $\rho g H S_o$) can be related for areas of constant depth (Abril, 2001), the average scaled secondary flow term, Γ^*_{ave}, can be expressed as

$$\Gamma^*_{ave} = \rho g S_o (1-k) \tag{4.20}$$

The calibrated values of *k* are 0.85 and 1.25, for the main channel and floodplain respectively. This yields,

$$\Gamma_{mc} = 0.15H\rho g S_o \qquad \Gamma_{fp} = -0.25H\rho g S_o \tag{4.21a,b}$$

for overbank flow conditions. Similarly, for inbank flow,

$$\Gamma_{mc} = 0.05H\rho g S_o \tag{4.22}$$

The use of equations (4.21a,b) will require user identification of the floodplain and main channel regions i.e. top of bank markers. Implementing this approach in irregular channel geometries, with '*H*' as the local depth, will result in discontinuity of these functions across the floodplain - main channel boundaries. This discontinuity effect has previously been found to be insignificant (Abril, 2001).

4.4.5 Secondary flow term for meandering channels

This term is present for sinuosities greater than 1.0 and is described as,

$$\frac{(\sigma - 1.0)}{0.1} C_{uv} \frac{\partial}{\partial y}\left[\frac{q^2}{H}\right] \qquad 1.0 \le \sigma \le 1.1$$

$$C_{uv} \frac{\partial}{\partial y}\left[\frac{q^2}{H}\right] \qquad \sigma > 1.1$$

(4.23a,b)

Previous research (Ervine *et al*, 2000) has found that C_{uv} is dependent on planform channel sinuosity, relative depth and relative roughness, and is generally in the range 0-5% in the main channel, and zero on the floodplain. This research incorporated an analytical solution that was section based, specifying continuity of the local velocity and velocity gradient at the vertical section interfaces. The numerical solution employed within the Conveyance Generator has identified the critical influence of the depth gradient (within the C_{uv} term) on laterally rising slopes. This term provides an over-estimation of the local unit flow and depth-averaged velocity, and hence the C_{uv} value should be set as zero on laterally rising slopes within the main channel. As no robust relationship has been established, the Conveyance Generator will incorporate a single C_{uv} value for the main channel (except for laterally rising slopes), which increases from 0% (straight channels) to ±10% (fully meandering channels). The sign of the C_{uv} value represents the direction of the meander, and will be assigned a negative or positive value. This will require the user to identify the bank top panel marker as the inner or outer part of the bend. User guidelines will be provided in the Conveyance Manual, which is the deliverable for Task T7.

4.4.6 Graphical representation of calibration parameters

Figure 4.3 provides a graphical representation of the parameter variation across a typical cross-section, as described in sections 4.4.1-5. The selection of the four calibration coefficients is based on previous research and expert advice. These parameters are still under investigation and hence these distributions/terms may change (possibly be updated in the SP) with further research. This methodology aims to incorporate the most recent research and where knowledge gaps exist in the literature, expert advice has been sought.

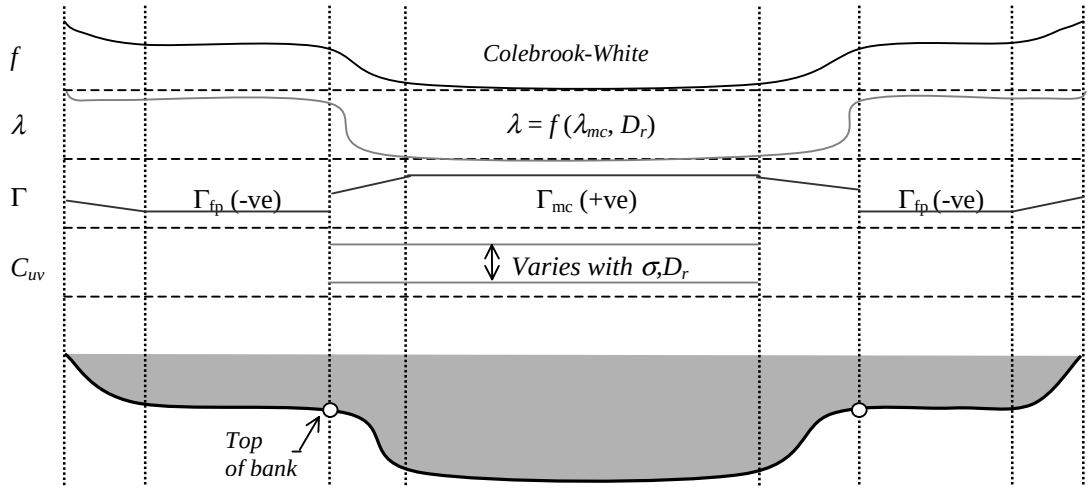

Figure 4.3 Lateral distribution of the calibration coefficients *f*, λ, Γ and C_{uv}

4.4.7 Discussion of parameters

The calibration coefficients λ and Γ have previously been determined within a finite element model (Abril, 2001) that solves for the depth-averaged velocity distribution, applying a Galerkin weighted residual method. This model does not incorporate the Colebrook-White friction law to evaluate the boundary friction *f*, which may result in the calibration parameters λ and Γ being marginally different within the Conveyance Generator.

The parameter assumptions are that:

(i) the friction slope S_f is approximated by the longitudinal bedslope S_o
(ii) the Colebrook-White friction law, with the coefficients for wide fully rough channels, is adequate for describing the distribution of f
(iii) λ can be expressed as a function of relative depth D_r and λ_{mc}
(iv) Γ is proportional to the stresses τ_{ave} and τ_d
(v) C_{uv} can be expressed as a direct function of the sinuosity
(vi) Γ and C_{uv} terms are both present for $1.0 < \sigma \leq 1.1$

4.5 Conclusion

Equations (4.8a,b) represent the form of the depth-integrated RANS to be incorporated in the Conveyance Generator. The various equation terms and parameters are described in accordance with 4.4.1-5. The associated assumptions are listed in Section 4.4.7. In addition, it should be recognised that the depth-averaged velocity and unit flow distributions that are predicted at high sinuosities, should be used with caution, unless determined at the meander apex.

The RANS approach and methodology outlined in this section satisfies the criteria cited in the Terms of Reference (Section 1.2),

- Develop selected method(s) to cover all cases of river/floodplain morphology. Ideally there should be a single unified method, with mechanism related terms which drop out or take zero values in various cases, determined by the measurable river system parameters.

The implementation of this method within the Conveyance Generator is detailed in Section 5.

5. IMPLEMENTATION OF SELECTED METHOD IN THE CONVEYANCE GENERATOR

5.1 Solution technique

This section describes the algorithm development for the Finite Element Method, which is the solution technique employed for equations (4.8a,b) within the Conveyance Generator.

5.1.1 Nature of the equation

Equations (4.8a,b) can be expressed in the more general form,

$$gHS_o - \frac{f\beta q^2}{8H^2} + \frac{\partial}{\partial y}\left[\lambda H\left(\frac{f}{8}\right)^{1/2} q \frac{\partial}{\partial y}\left(\frac{q}{H}\right)\right] = c_1\Gamma + c_2 C_{uv}\frac{\partial}{\partial y}\left[\frac{q^2}{H}\right] \tag{5.1}$$

Equation (5.1) is a non-linear, non-homogeneous, elliptic, second order partial differential equation, which requires either an analytical or numerical solution, as discussed in Section 3.3.1. The latter, in the form of a one-dimensional finite element solution that is well-suited to solution of elliptic equations, has been selected. This involves discretising the flow domain into a number of elements, and replacing the variable q with piecewise approximations, usually polynomials termed 'shape functions'. The result is a system of equations, which can be assigned boundary values and solved iteratively.

For application in one-dimensional channel flow, the solution domain is the cross-sectional area perpendicular to the flow direction. The domain is discretised through vertical slicing, generating fluid elements of width Δy. Each fluid element is in contact with the two adjacent elements, and the two elements situated at the cross-section edges are in contact with one other element and the boundary.

5.1.2 Linearising the system of equations

The equations are linearised by expressing the unit flow rate 'q' for iteration $n+1$ in terms of the unit flow rate of the previous iteration n,

$$q_{n+1} = q_n + \chi \Delta q_n \tag{5.2}$$

where: χ = relaxation factor in the range 0-1.5.
Δq_n = incremental change in q_n to improve the initial estimate

An initial estimate of q_n (based on the Manning equation) is made for the first iteration, and thereafter it is a known quantity. Substituting equation (5.2) into equation (5.1) and expressing the result as a system of linear equations for the solution of Δq_n, yields

$$\mathbf{M}[\Delta q_n] = \mathbf{x} \tag{5.3}$$

where **M** is the linear operator defined by

$$\mathbf{M}[\Delta q_n] = A\frac{\partial^2 \Delta q_n}{\partial y} + g(\frac{\partial \Delta q_n}{\partial y}, \Delta q_n, y) \tag{5.4}$$

and **x** is the vector of all contributing functions that are independent of Δq_n.

5.1.3 Piecewise functions (Davies, 1980)

The finite element method (FEM) provides an approximate solution for $\Delta q_n(y)$ through piecewise functions in a total of E elements. Thus for a general element i, an approximation is sought in such a manner that outside i,

$$\Delta q_{ni}(y) = 0 \qquad i = 1,...,E \tag{5.5}$$

and it follows that

$$\Delta q_n(y) = \sum_{E}^{i=1} \Delta q_{ni}(y) \tag{5.6}$$

Linear shape functions ϕ of the form (Figure 5.1),

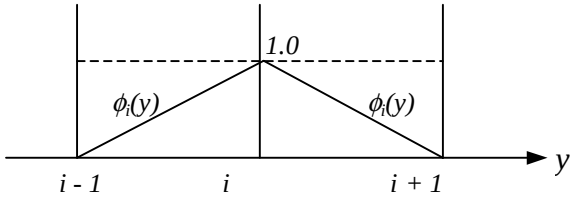

Figure 5.1 Linear shape functions for FEM analysis

are introduced where,

$$\Delta q_{ni}(y) = \sum \Delta q_{ni} \phi_i(y) \tag{5.7}$$

Similar approximations can be introduced to describe f, H and β distributions. Equation (5.3) is integrated over the flow domain R,

$$\int_R \mathbf{M}[\Delta q_n]\phi(y)\,dy - \int_R \mathbf{x}\phi(y)dy = 0 \tag{5.8}$$

and substituting the piecewise linear functions yields,

$$\sum_E \mathbf{M}\left(\sum \Delta q_{ni}\, \phi_i(y)\right)\phi_j(y) - \sum_E \left(\sum x_i\, \phi_i(y)\right)\phi_j(y) = 0 \tag{5.9}$$

Gauss-Legendre quadrature (Zienkiewicz, 1977), with two sampling points on each flow element, is the numerical integration method that is implemented. It is hence possible to evaluate Δq_n for each element, update q_n and repeat the procedure until a specified tolerance on Δq_n is satisfied.

5.1.4 Boundary conditions

A Dirichlet boundary conditions is imposed on the system of equations, i.e.

$$q = 0 \tag{5.10}$$

at the edge of the boundary elements.

5.1.5 Iteration strategy

To reduce the iteration requirement in achieving the solution tolerance, an approximate function for *f* at iteration *n+1*,

$$f_{n+1} = f_n + \frac{\partial f_n}{\partial q_n}\Delta q_n \tag{5.11}$$

is substituted into equation (4.8). The term $\partial f/\partial q$ is approximated through numerical differentiation (Newton's Method, 1964-71),

$$\frac{df}{dq} \approx \frac{f((1+p)\cdot q) - f(q)}{p \cdot q} \tag{5.12}$$

where the percentage p is in the range $0 < p \leq 0.5\%$.

5.2 Conveyance Generator

The Conveyance Generator comprises the computational code for solution of the system of equations developed in Section 5.1. The program language used was Microsoft Visual Basic V6.0 (2000), which was originally selected on the basis of an interactive Excel spreadsheet environment, i.e. Visual Basic for applications. As the spreadsheet environment was not employed, this code may be rewritten in a more computationally efficient language, e.g. Fortran or C++, at a later stage

The structure of the program is best described by means of a flow chart (Appendix 2). It provides an iterative solution to the systems of equations developed in 5.1, and hence solves for some additional output variables.

The Conveyance Generator inputs are the:

- cross-section topography i.e. surveyed height and offset distance
- reach average longitudinal bedslope S_o
- absolute roughness size k_s
- temperature T (can be single/seasonal/monthly value - default 15°C)
- sinuosity σ (thalweg length over valley length)
- top of bank markers to indicate bankfull (Γ distribution)
- top of bank markers indicating inner/outer meander bend (C_{uv} distribution)

Further guidance on these input parameters will be provided in the Conveyance Manual, which is the key deliverable for Task T7 of the Targeted Program. The Conveyance Generator outputs for the whole cross-section, which are given at every depth, are the:

- total flow rate Q (m^3/s)
- area A (m^2)
- average velocity U_{ave} (m/s)
- conveyance K (m^3/s)
- Froude Number Fr ($=\frac{u}{\sqrt{gR_m}}$ and R_m = hydraulic mean depth or ratio of area to surface width)
- Reynolds Number Re ($=\frac{uR_h}{\nu}$ and R_h is the hydraulic radius)
- Coriolis (or 'energy') coefficient α
- Boussinesq (or 'momentum) coefficient β_m
- surface water width B (m).

and for each depth, the lateral variation of the following variables is given:

- y co-ordinate (distance across channel section)
- z co-ordinate (i.e. channel bed profile)
- unit flow q (m^2/s)
- depth-averaged velocity U_d (m/s)
- unit conveyance k (= K/m) (m^2/s)
- shear velocity U_* (m/s)
- bed shear stress τ_b (N/m^2)
- bed friction f
- dimensionless eddy viscosity λ
- secondary flow term Γ

Further output options may include the above variables calculated separately for flow above the floodplain and main channels respectively e.g. U_{ave}, A, Fr, Re, α, β_m etc.

The Conveyance Generator handles braided river sections through treating each parallel channel as a separate unit and evaluating the flow for each. These individual channel flows can hence be summed to find the total flow (fig 5.2). The assumption is that the parallel channels have equal depths, bed/friction slopes, sinuosity and temperature for a given flow rate.

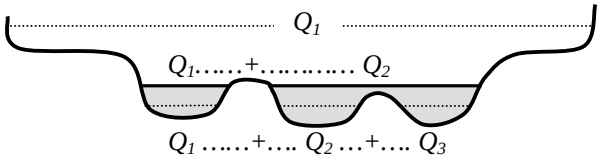

Figure 5.2 Addition of flow in braided channels

Storage areas or regions of zero flow should be handled through adjusting the boundary friction factor '*f*'. This would require increasing the input k_s value sufficiently, such that no flow occurs.

5.3 Open channel flow characteristics

This section provides a brief review of the typical open channel flow behaviour that the Conveyance Generator aims to predict.

5.3.1 Straight channels with inbank flow

The primary output of the Conveyance Generator is the stage-conveyance curve for a given cross-section geometry and roughness. The stage-discharge relationship can be obtained from equation (2.3),

$$K = \frac{Q}{S_f^{1/2}} \tag{2.3}$$

provided the reach average longitudinal bedslope, or alternatively the water surface slope, can be estimated within 10% of the actual value (Section 7.2.5). The conveyance capacity of a channel generally increases with water depth, at an increasing rate, as depicted in Figure 5.3. As the water level rises, the average channel width increases, and hence the area through which the fluid is conveyed.

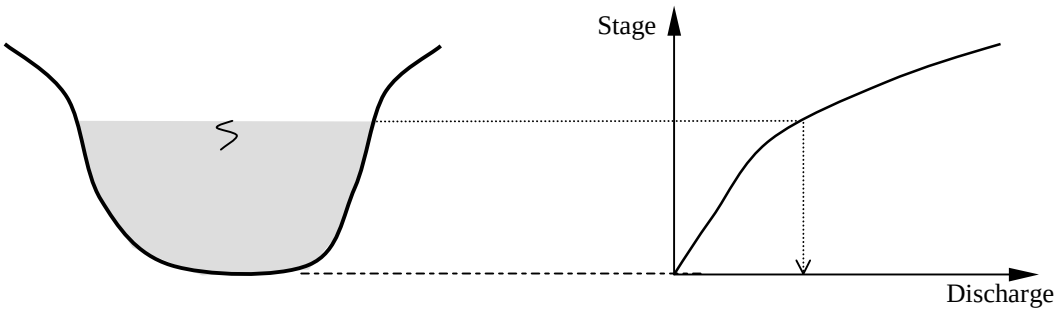

Figure 5.3 Stage-discharge curve for a simple channel cross-section

In addition (Section 5.2), the Conveyance Generator provides the lateral distribution of the unit flow rate q (m^2/s), the depth-averaged velocity U_d (m/s) and the bed shear stress τ_b (N/m^2) across a section. The unit flow has a value of zero at the channel edge/bank, and increases to a maximum near the channel centre, as the retarding effects of the boundary layer have less influence (Figure 5.4). The local streamwise velocity values are zero along the channel perimeter and they increase to a maximum value just below the water surface. Intuitively, the maximum value of the depth-averaged velocity occurs near the channel centre (Figure 5.4).

In an infinitely wide channel, with uniform flow conditions, the shear stresses increase from a value of zero at the water surface, to a maximum at the channel bed, according to

$$\tau = \rho g S_f (H - y) \approx \rho g S_o (H - y) \tag{5.13}$$

where y (m) is the depth measured from the channel bed. The bed shear stress is thus dependent on the local friction f and the local depth H, and a sudden change in either of these variables will result in a sudden change in the bed shear stress. The depth variations are incorporated in the solution of the Colebrook-White equation, and the CG can further handle local roughness values (k_s) provided by the Roughness Advisor, due to the discretisation of the channel cross-section.

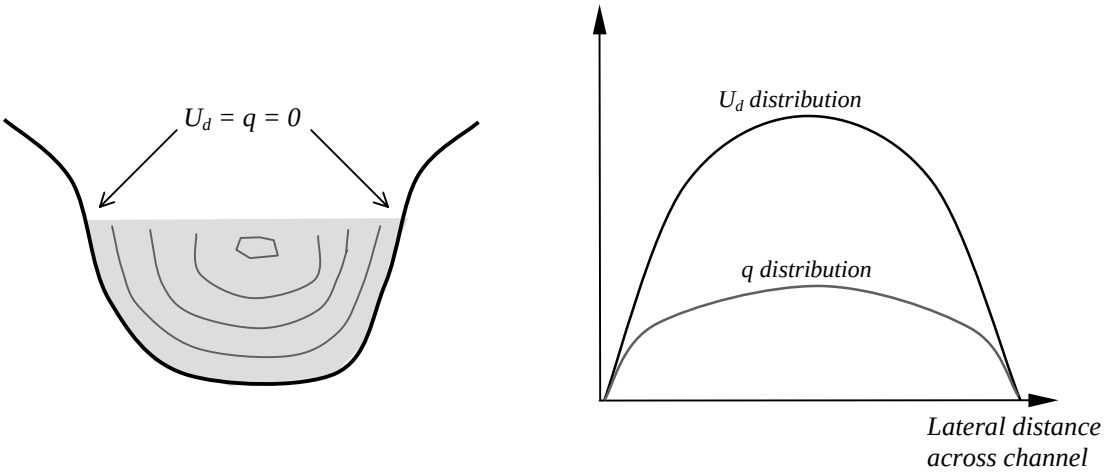

Figure 5.4 Lateral distribution of depth-averaged velocity and unit flow (for depth < 1.0 m)

5.3.2 Straight channels with overbank flows

In two-stage channels, the flow processes are more complex. When the flow is contained within the main channel, i.e. inbank, secondary flow cells perpendicular to the predominant flow direction develop (Figure 5.5). As the flow depth increases past bankfull, these secondary flow cells grow, and the flow passes onto the floodplains. At greater depths, secondary flow cells develop on the floodplain, which are oriented in the opposite direction to the reversed inbank circulation.

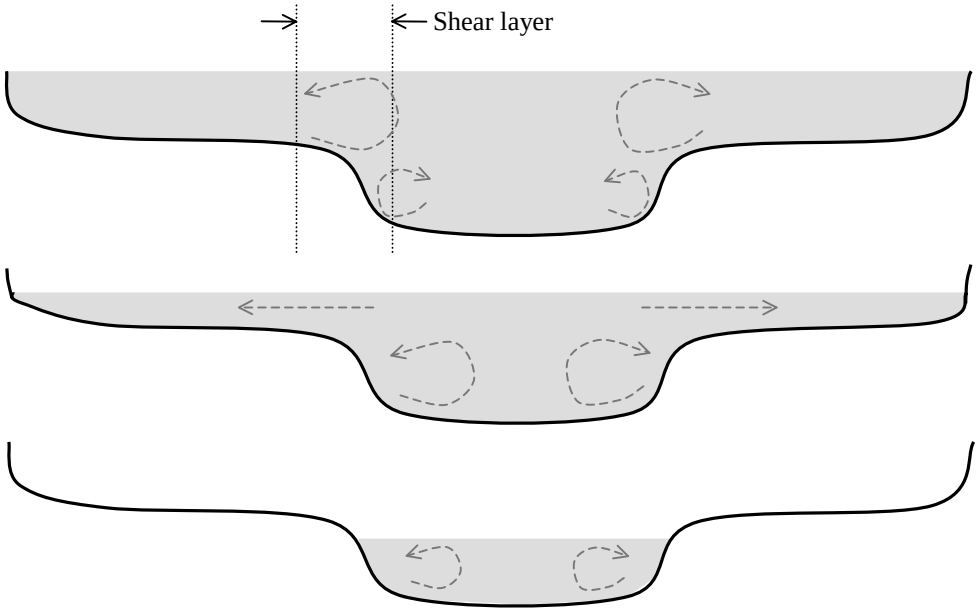

Figure 5.5 Secondary flow cells for two-stage channels

A steep velocity gradient occurs between the slow moving body of water on the floodplains and higher velocities in the main channel. This results in the dissipation of energy within this interaction zone termed the 'shear layer'.

5.3.3 Meandering channels

Meandering channels introduce a further degree of complexity to the flow features, including the development of helical secondary currents within the meander bends (see Shiono & Muto, 1998; Ervine *et al*, 2000; & for further details) and variations in cross-stream water levels. The resulting unit flow and depth-averaged velocity profiles are 'skewed' according to the direction of the meander bend, the position along the bend and the relative depth. For flow at the apex of a bend (sections AA & BB) and the cross-over region (section CC), Figure 5.6 illustrates previously observed depth-averaged velocity profiles.

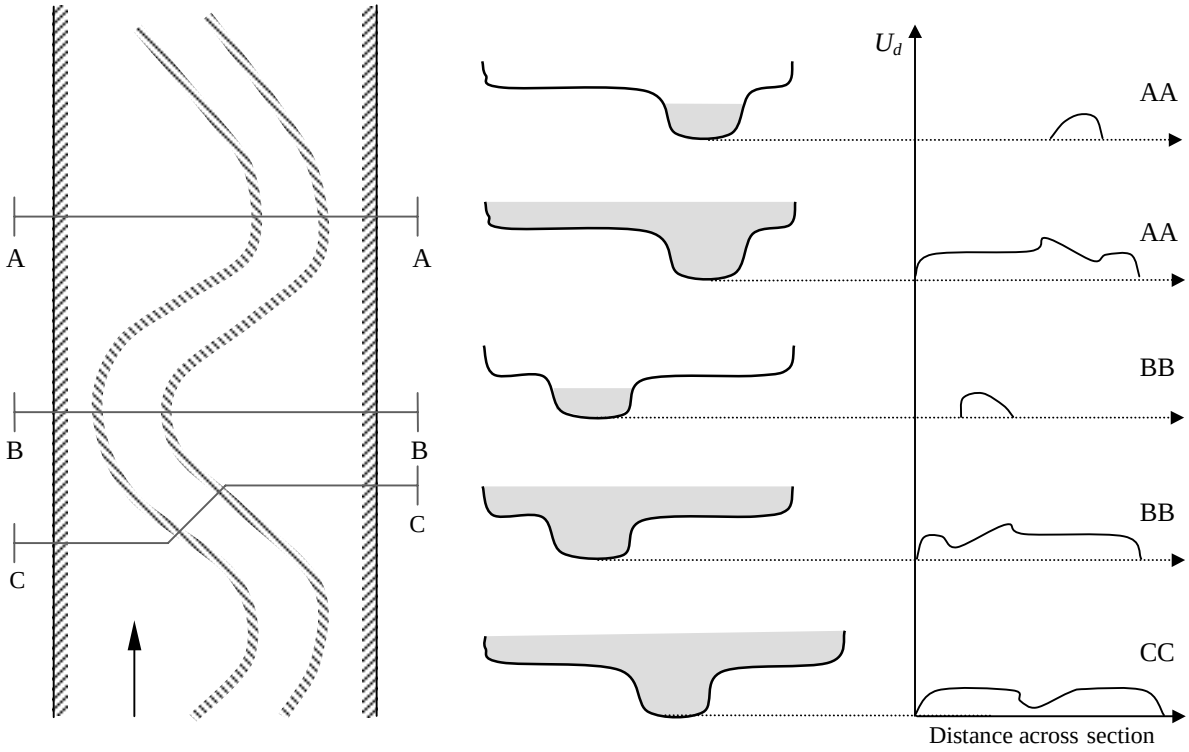

Figure 5.6 Depth-averaged velocity profiles in meandering channels

5.4 Conclusion

The Finite Element Approach has been implemented to solve the system of equations developed in Section 4. The Conveyance Generator, essentially a piece of code to facilitate the numerical iteration process, has been briefly described. Features of this program such as depth divisions, optimum lateral division of the elements, seasonal temperature variations etc. have not yet been included. The intention is to provide a simple, robust code that can be suitably tailored once the hydraulic calculation is adequate. Typically observed flow behaviour for simple, compound and meandering channels has been briefly discussed to aid interpretation of the CG results. Section 6 describes the testing of this code against physical models and purpose-made real river measurements.

6. TESTING OF THE CONVEYANCE GENERATOR

The Conveyance Generator was tested against the data sets identified in Interim Report 1: Data Mining, the deliverable for Task T1 of the Targeted Programme. This report identified four data categories,

- small scale flume data
- large scale flume data
- river measurements purpose-made for research
- real river data and corresponding 1D consultants models (Environment Agency Section 105 & MDSF models)

of which the first three categories are employed in the initial testing phase. Only once both the Roughness Advisor and the Conveyance Generator are incorporated in the CES, will it be feasible to test the real river data, for which advice is sought regarding the vegetation type, occurrence and associated roughness value.

6.1 Data description

This section provides a brief review of the data sets and the conditions under which they were recorded. It includes a flume/channel description, typical flow rates, which flow parameters were observed and the reliability of/confidence in these measurements.

6.1.1 Flood Channel Facility (FCF) data

A managed programme of research on the EPSRC Flood Channel Facility (FCF) at HR Wallingford Ltd. has provided a valuable data set, covering a range of flow conditions. The large-scale test flume was 56m long, 10m wide and 0.4m deep with an average bedslope of 0.01. The main channel geometries included rectangular, trapezoidal and pseudo natural shapes, while the floodplains were varied with respect to width and roughness. Water was fed into the flume by six pumps, with a combined capacity of $1.08m^3/s$. At the inlet, the water flowed over a sharp-crested weir and into a stilling pool, before spilling onto the floodplains and into the main channel. Five separate tailgates at the downstream end were used to control the surface slope and depth of water in the model. Further details in FCF Reports (HR Wallingford Report SR314).

The first testing phase, Phase A, examined straight prismatic channels (Series 1-13), including both symmetric and asymmetric cases, as well as skewed channels (Series 14-19) at 2.1, 5.1 and 9.2 degrees to the streamwise floodplain direction. The Phase B experiments were designed to investigate meandering channels of both 60 and 100 degree bends (Figure 6.1).

The measurements taken include:

- velocity magnitude and angle (vane attached to a rotary potentiometer)
- discharge (orifice plate meters)
- water surface levels (manual pointer gauges in stilling wells)
- boundary shear stresses (Preston tube)
- turbulence observations (laser doppler system TSI model 9273)

These large-scale flumes, sophisticated equipment and measurement techniques have ensured the highest quality data. Thus the FCF data is considered to be of better quality than any other model data in the world (Ervine, Scoping Study Annex).

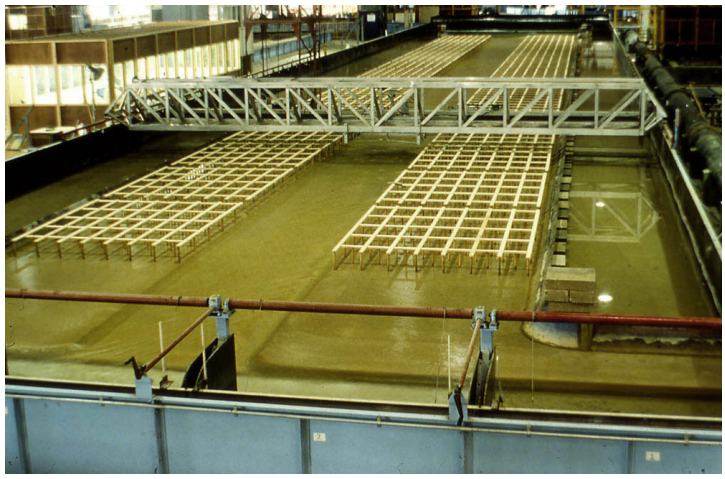

(a)

(b)

(c)

Figure 6.1 FCF experimental flumes for (a) & (b) Phase A straight channels and (c) Phase B meandering channels

6.1.2 Glasgow data

The Glasgow small-scale flume was a scaled model of the FCF configuration, with a reduction factor of 6 (Figure 6.2). This enabled the meander belt width and wavelength to be incorporated with enough wavelengths to ensure fully developed flow. The flume was 8m long, 1.65m wide, with an average slope of 1:1000 and it included 3.5 wavelengths. The channel bed was constructed from polystyrene sheets, attached to the bed with silicon gel. The main channel, approximately 0.2m wide, was investigated for rectangular, trapezoidal and quasi-natural shapes. The observed flow parameters included stage, velocity and discharge.

Figure 6.2 The Glasgow experimental flume

This data set is typical of the meticulously measured and recorded university measurements for the purpose of academic research. The data is strong in both quality and quantity (Ervine, Scoping Study Annex).

6.1.3 Blackwater 1:5 scale model

The River Blackwater (Hampshire, UK) 1:5 scale model was reproduced in the FCF at HR Wallingford. It is unusual in that it provides a doubly sinuous compound channel flow case i.e. both the main channel and floodplain are meandering, but with different sinuosities. The model was moulded with cement mortar and the water was supplied through three pipes at the inlet with a maximum discharge capacity of $0.25m^3/s$. As with the FCF measurements, the water level was controlled by downstream tailgates. Figure 6.3 illustrates the testing facility.

The measurements taken include:

- discharge (orifice plates)
- velocity, overbank velocity (rotary potentiometer)
- water level
- friction slopes

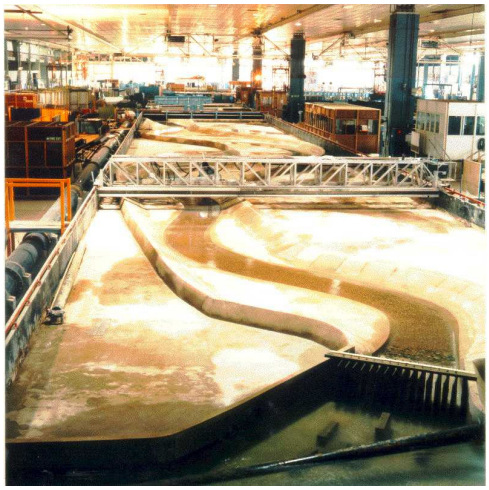

Figure 6.3 1:5 scale model of the River Blackwater at HR Wallingford Ltd.

This high quality data set has the added advantage of real river measurements for comparison and determining the effects of scale.

6.1.4 River Main

The River Main, situated in Ulster, Northern Ireland, has a mean annual flow of $0.5m^3/s$ and a mean annual flood of $65m^3/s$ (Hydrological Data UK, 1998).

An 800m long reach has been closely monitored (Myers, 1990), as part of an experimental program carried out on a section that was reconstructed to form a compound channel. The reach is essentially straight, with one 45 degree bend. The top width is 14m, the total width inclusive of floodplains varies in the range 27.3-30.4m, and bankfull depth is approximately 0.9-1.0m. The floodplains slope towards the main channel with a 1:25 gradient and the longitudinal slope is 1:520. The river bed consists of coarse gravel with a d_{50} of 10-20mm. The main channel side slopes consist of quarry stone and the berms are covered with heavy weed growth. Figure 6.4 shows the study area.

(a) (b)

Figure 6.4 River Main in County Antrim, Northern Ireland (a) the cobbled side-banks and (b) a gentle meander

The measured data for nine consecutive cross-sections spaced approximately 100m apart includes:

- discharge (collected at a bridge on the upstream end of the reach)
- water level
- velocity (final cross-section only)

The stage-discharge measurements were improved by dividing the channel into three, by means of vertical (zero stress) surfaces placed above the inner banks.

6.1.5 River Severn

The River Severn is third longest river in Britain, after the Derwent and the Wye. It measures an estimated 206km in length and has a mean annual discharge of 62.7m^3/s (Babaeyan-Koopaei *et al*, 2002).

Montford

The River Severn at Montford had been extensively monitored for research purposes, providing a large body of accurate current metering data.

(a) (b)

Figure 6.5 River Severn at Montford (a) looking upstream from right bank (b) looking downstream from cableway

This is a natural section with a cableway extending over the full width including the floodplains. The bankfull width and depth are 40m and 6.3m respectively. The total width, including the floodplains, is approximately 120m and the longitudinal slope is 1:5128. The floodplains are grass-covered (Figure 6.4) and the gauged station is on a straight section of the river.

The measured data includes water levels, velocity and discharge.

Shrewsbury

A reach of the River Severn, 20km east of Shrewsbury, has been monitored for flow measurements purpose-made for research. A single meander about 600m long, located south of Llandrinio near Lower Farm, was the selected site. The main channel is 30m wide, 6-7m deep with respect to the upstream right floodplain (180m wide, 120m long) and 9m deep with respect to the higher downstream floodplain situated on the left. The longitudinal bedslope is 1:6850 (Babaeyan-Koopaei *et al*, 2002).
Detailed measurements of:

- velocity (acoustic doppler velocity ADV & cable supported directional current meter)
- tubulence (3D ADV)

were recorded immediately downstream of the single meander.

6.1.6 River Blackwater

The River Blackwater in Hampshire, UK, has been extensively monitored in terms of flow parameters, vegetation growth patterns and channel deformation (Sellin R. personal communication). In 1993, a 3km length of the Blackwater was reconstructed as a doubly meandering two-stage trapezoidal channel, with a main channel and floodplain sinuosity of 1.18 and 1.05 respectively. It is capable of carrying the 100year flood, 4.3m^3/s, and an upstream spillway ensures that the flow does not exceed 4m^3/s.

Figure 6.6 Vegetation on the River Blackwater (Hampshire, UK)

The instrumented reach is 520m long, serves a 40km^2 catchment and responds to local storms. The main channel width is 425m and the average berm width is 490m (Sellin &

van Beesten, 2002). The inbank vegetation builds up in the summer (Figure 6.5) and is washed out in Autumn, while the out-of-bank vegetation is cut in October.

The measured flow parameters were:

- stage
- discharge (upstream: electromagnetic gauge; within reach: electric coils with pressure transducers connected by tubes to river)
- calculated output: change in Manning;s *n* with season

The measurements achieve good accuracy for high flows, but are less accurate at low flows.

6.2 Testing

This section describes the test results for the data sets presented in Section 6.1. These results are described in three categories: (i) straight prismatic channels (ii) channels with some degree of skew and (iii) fully meandering channels. All figures appear in Appendix 3.

6.2.1 Straight channels

(i) FCF Phase A data

The FCF phase A series 2 (out-of-bank) and series 4 (inbank) results were predicted by the Conveyance Generator. Figure 6.7 illustrates the cross-section trapezoidal geometry, with the top of bank panel markers indicated with two small circles. The input parameters for the model are summarised in Table 6.1.

Table 6.1 FCFA Series 2 & 4 model/input parameters

Parameter	Default Value	Value Used
Reach average longitudinal bedslope S_o	0.001	0.001027
Absolute roughness height k_s (m) (1) main channel (2) floodplain	RA / RHS*	 0.00014 0.00014
Equivalent n_l (1) main channel (2) floodplain	RA / RHS	 0.00866 0.00866
Colebrook-White equation coefficients (details Table 4.2) (1) laboratory/engineered channel, trapezoidal, smooth (2) laboratory/engineered channel, trapezoidal, rough (3) Real rivers/natural channels		(1)
Main channel dimensionless eddy viscosity (λ_{mc})	0.24	✓
Inbank secondary flow coefficient (Γ_{imc})	+0.050	✓
Main channel out-of-bank secondary flow coefficient (Γ_{omc})	+0.150	✓
Floodplain out-of-bank secondary flow coefficient (Γ_{ofp})	-0.250	✓
Sinuosity σ	0	✓
Meandering secondary flow coefficient (% C_{uv}) (1) inbank (2) out-of-bank	 0 0	 ✓ ✓
Temperature of fluid (T °C)	15	✓
Top of bank panel markers present		✓

*RA Roughness Advisor – component of CES providing local roughness values
*RHS River Habitat Survey - a standard method for capturing data on the physical habitat of rivers, which includes 20 000 sites in the United Kingdom and elsewhere. Part of this will be incorporated in the RA, for cases where there is limited site knowledge.

The stage-discharge relationships for series 4 & 2 are shown in Figure 6.8 & 6.9 respectively. The CG results predict the observed measurements with good accuracy. The depth-averaged velocity (Figures 6.10-15), the unit flow rate (Figures 6.16-21) and the bed shear stress (Figures 6.22-27) lateral distributions for six different depths of

flow are compared to the observed data. The selected depths include 2 inbank and 4 out-of-bank flow cases. In general, the predicted velocities and unit flow rates compare well to the data; however, just above bankfull (0.15m), i.e. at depth = 0.16873 (in Figure 6.18), the main channel discharge is slightly under-predicted. This is anticipated from the stage-discharge curve (Figure 6.9) where the 'best-fit' overall curve marginally under-predicts the total flow just above bankfull. The bed shear stresses are less accurately predicted for the lower depths, however, at greater depths the results are reasonable. The 'spikes' that are present at the channel edges and interface between the main channel and floodplain are expected due to the abrupt change in the Darcy *f* value (solution of the Colebrook-White equation). Further details in Section 5.3.1.

(ii) River Main

The stage-discharge relationship for two sections on the River Main were predicted by the CG. Section 6 is upstream of the reach and section 14 is 800m further downstream. Figures 6.28 & 6.29 illustrate the trapezoidal cross-section geometries. Tables 6.2 & 6.3 summarise the model input data for the two sections respectively. The difference between the input parameters for the two-sections is that the absolute roughness values are lower for the downstream section, as previously found by Ackers (1993) and Wark (1993).

Table 6.2 River Main Section 6 model/input parameters

Parameter	**Default Value**	**Value Used**
Reach average longitudinal bedslope S_o	0.001	0.001906
Absolute roughness height k_s (m) (1) main channel (2) floodplain	RA / RHS	 0.3566 0.5131
Equivalent n_l (1) main channel (2) floodplain	RA / RHS	 0.032 0.034
Colebrook-White equation coefficients (details Table 4.2) (1) laboratory/engineered channel, trapezoidal, smooth (2) laboratory/engineered channel, trapezoidal, rough (3) Real rivers/natural channels		(3)
Main channel dimensionless eddy viscosity (λ_{mc})	0.24	✓
Inbank secondary flow coefficient (Γ_{imc})	+0.050	✓
Main channel out-of-bank secondary flow coefficient (Γ_{omc})	+0.150	✓
Floodplain out-of-bank secondary flow coefficient (Γ_{ofp})	-0.250	✓
Sinuosity σ	0	✓
Meandering secondary flow coefficient (% C_{uv}) (1) inbank (2) out-of-bank	 0 0	 ✓ ✓
Temperature of fluid (T °C)	15	✓
Top of bank panel markers present		✓

Table 6.3 River Main Section 14 model/input parameters

Parameter	Default Value	Value Used
Reach average longitudinal bedslope S_o	0.001	0.001906
Absolute roughness height k_s (m) (1) main channel (2) floodplain	RA / RHS	 0.0811 0.1600
Equivalent n_l (1) main channel (2) floodplain	RA / RHS	 0.025 0.028
Colebrook-White equation coefficients (details Table 4.2) (1) laboratory/engineered channel, trapezoidal, smooth (2) laboratory/engineered channel, trapezoidal, rough (3) Real rivers/natural channels		(3)
Main channel dimensionless eddy viscosity (λ_{mc})	0.24	✓
Inbank secondary flow coefficient (Γ_{imc})	+0.050	✓
Main channel out-of-bank secondary flow coefficient (Γ_{omc})	+0.150	✓
Floodplain out-of-bank secondary flow coefficient (Γ_{ofp})	-0.250	✓
Sinuosity σ	0	✓
Meandering secondary flow coefficient (% C_{uv}) (1) inbank (2) out-of-bank	 0 0	 ✓ ✓
Temperature of fluid (T °C)	15	✓
Top of bank panel markers present		✓

The stage-discharge predictions for these two sections are compared to the observed data in Figures 6.30 and 6.31 respectively. The inbank predictions for Section 6 are good. However, above bankfull the flow is slightly under-predicted and at much greater depths the curve moves away from the measured values, resulting in an over-estimation of the discharge. This trend cannot be altered through adjusting the roughness values, as increased floodplain roughness would further reduce the discharge above bankfull, while possibly correcting the flow at greater depths.

The stage-discharge curve for section 14 predicts the data very well, except at great depths. This is possibly due to a much higher roughness on the extreme floodplain edges, the values of which are not documented. These values may be available through the Roughness Advisor at a later stage.

The depth-averaged velocity distribution for a depth of 1.37m in section 14 was predicted. Figure 6.32 shows the comparison to the measured data. The velocity data matches the measured data with reasonable accuracy, however, it appears that the left floodplain roughness has been under-estimated and the main channel flow is slightly over-estimated. The predicted total flow rate for this depth was 35.26m^3/s and the measured flow rate was 36.05m^3/s, i.e. within 2.2% of the actual value.

(iii) River Severn (Montford)

The River Severn data measurements at Montford Bridge were predicted by the CG. The cross-section geometry is depicted in Figure 6.33. The model input parameters are tabulated below (Table 6.4).

Table 6.4 River Severn at Montford Bridge model/input parameters

Parameter	**Default Value**	**Value Used**
Reach average longitudinal bedslope S_o	0.001	0.0002
Absolute roughness height k_s (m) (1) main channel (2) floodplain	RA / RHS	 0.2420 0.6105
Equivalent n_l (1) main channel (2) floodplain	RA / RHS	 0.030 0.035
Colebrook-White equation coefficients (details Table 4.2) (1) laboratory/engineered channel, trapezoidal, smooth (2) laboratory/engineered channel, trapezoidal, rough (3) Real rivers/natural channels		(3)
Main channel dimensionless eddy viscosity (λ_{mc})	0.24	✓
Inbank secondary flow coefficient (Γ_{imc})	+0.050	✓
Main channel out-of-bank secondary flow coefficient (Γ_{omc})	+0.150	✓
Floodplain out-of-bank secondary flow coefficient (Γ_{ofp})	-0.250	✓
Sinuosity σ	0	✓
Meandering secondary flow coefficient (% C_{uv}) (1) inbank (2) out-of-bank	 0 0	 ✓ ✓
Temperature of fluid (T °C)	15	✓
Top of bank panel markers present		✓

Figure 6.34 illustrates the stage-discharge predictions for both inbank and out-of-bank flows. The results compare favourably to the measured data, in particular capturing the variations at bankfull through the secondary flow terms.

The depth-averaged velocity measurements were predicted for depths of 6.92m and 7.81m (see Figures 6.35 & 6.36 respectively). At depth 6.92m, the velocity distribution corresponds well to the measured data. The data measurements that appear to be beyond the extent of the wetted area arise from the discrepancies between the available survey data and the true section geometry at the time of measuring. The slight rise in the velocity at the channel edges is expected. The CG solves for the unit flow rate q, which rapidly reduces towards the channel edge, while the local depth also reduces but less rapidly towards the channel edge (Figure 6.33). The depth-averaged velocity is determined through $U_d = qH$ and the result is the rise in velocity just prior to the channel bank. The predicted discharge was 227.92m^3/s and the measured flow was 229.8m^3/s i.e. within 1% of the actual value.

The depth-averaged velocity distribution for a depth of 7.81m appears to over-estimate the velocities on the left floodplain and in the centre of the main channel. This distribution can be improved by altering the roughness values, however, the result is a

less accurate flow rate. The predicted discharge was 334.353m^3/s and the measured flow was 334.1m^3/s i.e. within 0.1% of the actual value.

6.2.2 Channels with some degree of skew

FCF phase A Series 14 & 15 data has been predicted with the Conveyance Generator. Series A14 and A15 represent channels that are skewed relative to the floodplain by an angle of 5 and 9 degrees respectively. The stage-discharge relationship was measured mid-reach, i.e. where the section is approximately symmetrical (Figure 6.37). Velocity measurements were taken at sections upstream (Figure 6.38 & 6.40) and downstream (Figure 6.39 & 6.41) for the two cases respectively. The model input parameters are summarised in Tables 6.5 & 6.6. The equivalent channel sinuosity for a 5 and 9 degree skew is 1.0038 and 1.012. These values are in the range 1.0-1.1, where both the straight (Γ) and sinuous (C_{uv}) secondary flow terms are present.

Table 6.5 FCFA Series A14 model/input parameters

Parameter	Default Value	Value Used
Reach average longitudinal bedslope S_o	0.001	0.001207
Absolute roughness height k_s (m) (1) main channel (2) floodplain	RA / RHS	 0.00005 0.00005
Equivalent n_l (1) main channel (2) floodplain	RA / RHS	 0.007 0.007
Colebrook-White equation coefficients (details Table 4.2) (1) laboratory/engineered channel, trapezoidal, smooth (2) laboratory/engineered channel, trapezoidal, rough (3) Real rivers/natural channels		(1)
Main channel dimensionless eddy viscosity (λ_{mc})	0.24	✓
Inbank secondary flow coefficient (Γ_{imc})	+0.050	x 0.5
Main channel out-of-bank secondary flow coefficient (Γ_{omc})	+0.150	x 0.5
Floodplain out-of-bank secondary flow coefficient (Γ_{ofp})	-0.250	x 0.5
Sinuosity σ	0	1.0038
Meandering secondary flow coefficient (% C_{uv}) (1) inbank (2) out-of-bank	 0 0	 -0.5 -0.5
Temperature of fluid (T °C)	15	✓
Top of bank panel markers present		✓

Table 6.6 FCFA Series A15 model/input parameters

Parameter	Default Value	Value Used
Reach average longitudinal bedslope S_o	0.001	0.001207
Absolute roughness height k_s (m) (1) main channel (2) floodplain	RA / RHS	 0.00005 0.00005
Equivalent n_l (1) main channel (2) floodplain	RA / RHS	 0.007 0.007
Colebrook-White equation coefficients (details Table 4.2) (1) laboratory/engineered channel, trapezoidal, smooth (2) laboratory/engineered channel, trapezoidal, rough (3) Real rivers/natural channels		(1)
Main channel dimensionless eddy viscosity (λ_{mc})	0.24	✓
Inbank secondary flow coefficient (Γ_{imc})	+0.050	x 0.25
Main channel out-of-bank secondary flow coefficient (Γ_{omc})	+0.150	x 0.25
Floodplain out-of-bank secondary flow coefficient (Γ_{ofp})	-0.250	x 0.25
Sinuosity σ	0	1.012
Meandering secondary flow coefficient (% C_{uv}) (1) inbank (2) out-of-bank	 0 0	 -0.75 -0.75
Temperature of fluid (T °C)	15	✓
Top of bank panel markers present		✓

The stage-discharge results for the mid-reach sections are depicted in Figures 6.42 and 6.43. The predictions match the measured data well, except for the region just above bankfull. This is possibly due to the depth at which the transition from the inbank to the overbank secondary flow terms occurs, which is set at bankfull, but possible should be implemented just above bankfull. Research to date does not provide a preferred option.

The depth-averaged velocity distributions for the upstream and downstream cross-sections of the 5 degree skew channel at depth 0.17606m are presented in Figures 6.44 & 6.45. The measured flow rate for this depth is 0.261m^3/s and the predicted values were 0.2597m^3/s (upstream) and 0.2596m^3/s (downstream). The upstream velocity matches the data fairly well, except for the left bank. The velocities are over-estimated, however, the flow rates correspond. This could indicate instantaneous high velocities, while in truth, the time-averaged velocities are lower. The downstream velocities correspond well to the measured data.

The depth-averaged velocities at a depth of 0.1978m were predicted for the 9 degree skew channel. The measured flow rates was 0.3557 m^3/s, and the predicted values were 0.3456m^3/s (upstream) and 0.3460m^3/s (downstream) i.e. under-predicting by approximately 2.8%. This is apparent in the velocity distributions (Figure 6.46 & 6.47), where the Conveyance Generator fails to predict the increased velocity and skew on the left floodplain, as C_{uv} is zero on the floodplains. However, the main channel and right floodplain velocities were well predicted.

6.2.3 Fully meandering channels

(i) Glasgow data

The Glasgow University data set was used to test the CG predictions for meandering channels in small-scale flumes. Two cases were selected, G75T90S, i.e. smooth channels with 90 degree main channel side walls, and G25T45S, i.e. smooth channel with 45 degree main channel side slopes (Figures 6.48 & 6.49). The model input parameters are summarised in Tables 6.7 and 6.8. In general, the C_{uv} values are lower for inbank flows, and the sign is the opposite to overbank flow, due to the reversed direction of skew.

Table 6.7 Glasgow experiment Series G75T90S model/input parameters

Parameter	**Default Value**	**Value Used**
Reach average longitudinal bedslope S_o	0.001	0.001
Absolute roughness height k_s (m) (1) main channel (2) floodplain	RA / RHS	 0.003 0.003
Equivalent n_l (1) main channel (2) floodplain	RA / RHS	 0.014 0.014
Colebrook-White equation coefficients (details Table 4.2) (1) laboratory/engineered channel, trapezoidal, smooth (2) laboratory/engineered channel, trapezoidal, rough (3) Real rivers/natural channels		(1)
Main channel dimensionless eddy viscosity (λ_{mc})	0.24	✓
Inbank secondary flow coefficient (Γ_{imc})	+0.050	0
Main channel out-of-bank secondary flow coefficient (Γ_{omc})	+0.150	0
Floodplain out-of-bank secondary flow coefficient (Γ_{ofp})	-0.250	0
Sinuosity σ	0	1.374
Meandering secondary flow coefficient (% C_{uv}) (1) inbank (2) out-of-bank	 0 0	 -0.9 3.0
Temperature of fluid (T °C)	15	25
Top of bank panel markers present		✓

Table 6.8 Glasgow experiment Series G25T45S model/input parameters

Parameter	Default Value	Value Used
Reach average longitudinal bedslope S_o	0.001	0.001
Absolute roughness height k_s (m) (1) main channel (2) floodplain	RA / RHS	 0.001-0.002 0.001-0.002
Equivalent n_l (1) main channel (2) floodplain	RA / RHS	 0.012-0.0135 0.012-0.0135
Colebrook-White equation coefficients (details Table 4.2) (1) laboratory/engineered channel, trapezoidal, smooth (2) laboratory/engineered channel, trapezoidal, rough (3) Real rivers/natural channels		(1)
Main channel dimensionless eddy viscosity (λ_{mc})	0.24	✓
Inbank secondary flow coefficient (Γ_{imc})	+0.050	0
Main channel out-of-bank secondary flow coefficient (Γ_{omc})	+0.150	0
Floodplain out-of-bank secondary flow coefficient (Γ_{ofp})	-0.250	0
Sinuosity σ	0	1.374
Meandering secondary flow coefficient (% C_{uv}) (1) inbank (2) out-of-bank	 0 0	 - 3.0-4.0
Temperature of fluid (T °C)	15	25
Top of bank panel markers present		✓

The inbank and out-of-bank stage-discharge predictions for Series G75T90S are shown in Figures 6.50 and 6.51 respectively. Both curves slightly under-predict the discharge, possibly due to the values of C_{uv} being on the high side. As the FCF Phase B data tests were undertaken first, the C_{uv} values for a sinuosity of 1.374 were pre-calibrated, and were thus not altered for this test. The stage-discharge prediction for Series G25T45S (out-of-bank flow) is shown in Figure 6.52. In this instance, the data is well predicted for the same value of C_{uv}.

The depth-averaged velocity for Series G25T45S depth = 0.042m at the bend apex is predicted in Figure 6.53. The velocity on the floodplains is under-predicted along with the amount of skew. The absolute roughness value was decreased to 0.001 and C_{uv} value was increased to 4%. This improved the velocity distribution (Figure 6.54), however, the corresponding stage-discharge curve (Figure 6.55) was less accurate. The measured flow rate for this depth was 0.00507m^3/s. The initial prediction was 0.00493m^3/s (i.e. 2.76% different) while the second prediction was 0.00532m^3/s (i.e. 4.93% different). As the stage-discharge curve is the primary output for the CG, the initial stage-discharge curve is more appropriate.

(ii) FCF Phase B data

The FCF Phase B data was used to calibrate the initial set of C_{uv} values for meandering channels. Most of Series 20-42 data was predicted using the CG. The three cross-section geometries used are shown in Figures 6.56, 6.57 and 6.58 and these correspond to Series B20-24, Series B25-30, and Series B38-42 respectively. The model input parameters are summarised in Tables 6.9-6.11.

Table 6.9 FCFB Series B20-24 model/input parameters

Parameter	Default Value	Value Used
Reach average longitudinal bedslope S_o	0.001	0.000996
Absolute roughness height k_s (m) (1) main channel (2) floodplain	RA / RHS	 0.0007 0.0007
Equivalent n_l (1) main channel (2) floodplain	RA / RHS	 0.011 0.011
Colebrook-White equation coefficients (details Table 4.2) (1) laboratory/engineered channel, trapezoidal, smooth (2) laboratory/engineered channel, trapezoidal, rough (3) Real rivers/natural channels		(1)
Main channel dimensionless eddy viscosity (λ_{mc})	0.24	✓
Inbank secondary flow coefficient (Γ_{imc})	+0.050	0
Main channel out-of-bank secondary flow coefficient (Γ_{omc})	+0.150	0
Floodplain out-of-bank secondary flow coefficient (Γ_{ofp})	-0.250	0
Sinuosity σ	0	1.374
Meandering secondary flow coefficient (% C_{uv}) (1) inbank (2) out-of-bank	 0 0	 -0.9 3.0
Temperature of fluid (T °C)	15	✓
Top of bank panel markers present		✓

Table 6.10 FCFB Series B25,26 & 30 model/input parameters

Parameter	Default Value	Value Used
Reach average longitudinal bedslope S_o	0.001	0.000996
Absolute roughness height k_s (m) (1) main channel (2) floodplain	RA / RHS	 0.0007 0.0007
Equivalent n_l (1) main channel (2) floodplain	RA / RHS	 0.011 0.011
Colebrook-White equation coefficients (details Table 4.2) (1) laboratory/engineered channel, trapezoidal, smooth (2) laboratory/engineered channel, trapezoidal, rough (3) Real rivers/natural channels		(1)
Main channel dimensionless eddy viscosity (λ_{mc})	0.24	✓
Inbank secondary flow coefficient (Γ_{imc})	+0.050	0
Main channel out-of-bank secondary flow coefficient (Γ_{omc})	+0.150	0
Floodplain out-of-bank secondary flow coefficient (Γ_{ofp})	-0.250	0
Sinuosity σ	0	1.374
Meandering secondary flow coefficient (% C_{uv}) (1) inbank (2) out-of-bank	 0 0	 -2.0 3.0
Temperature of fluid (T °C)	15	✓
Top of bank panel markers present		✓

Table 6.11 FCFB Series B38,39 & 42 model/input parameters

Parameter	Default Value	Value Used
Reach average longitudinal bedslope S_o	0.001	0.001021
Absolute roughness height k_s (m) (1) main channel (2) floodplain	RA / RHS	 0.0007 0.0007
Equivalent n_l (1) main channel (2) floodplain	RA / RHS	 0.011 0.011
Colebrook-White equation coefficients (details Table 4.2) (1) laboratory/engineered channel, trapezoidal, smooth (2) laboratory/engineered channel, trapezoidal, rough (3) Real rivers/natural channels		(1)
Main channel dimensionless eddy viscosity (λ_{mc})	0.24	✓
Inbank secondary flow coefficient (Γ_{imc})	+0.050	0
Main channel out-of-bank secondary flow coefficient (Γ_{omc})	+0.150	0
Floodplain out-of-bank secondary flow coefficient (Γ_{ofp})	-0.250	0
Sinuosity σ	0	2.04
Meandering secondary flow coefficient (% C_{uv}) (1) inbank (2) out-of-bank	 0 0	 -5.5 8.0-10.0
Temperature of fluid (T °C)	15	✓
Top of bank panel markers present		✓

The stage-discharge prediction for Series B20 (inbank) and B21 (out-of-bank) are shown in Figures 6.59 and 6.60 respectively. The predictions capture the curvature of the measured data very well for both cases. The depth-averaged velocities for depths of 0.2m and 0.25m were predicted (Figure 6.61 & 6.62) at the bend apex. The measured velocity data corresponds reasonably well. The measured flow rates were 0.2512m^3/s and 0.6344m^3/s and the calculated values were 0.2472m^3/s (i.e. 1.6% different) and 0.6268m^3/s (1.2% different).

The estimated stage-discharge curves for Series B25 (inbank) and B26 (out-of-bank) are shown in Figures 6.63 and 6.64. The discharge is slightly over-predicted above bankfull, and under-predicted at the lowest depth. The inbank C_{uv} value was increased to best-fit the data. This can be explained by the nature of the main channel cross-section shape (Figure 6.57). In Series B20 & 21, the main channel was trapezoidal. The result was that the C_{uv} had a non-zero value everywhere except for the side slope on the right of the channel. In the Series B25 & 26 geometry, the laterally rising slope is spread more evenly over the main channel, reducing the area where the C_{uv} value is non-zero. The result is that the meandering energy losses are under-predicted and the resulting discharge is over-predicted. The solution was thus to increase the C_{uv} value to 2%. The overbank flow stage-discharge prediction was based on the original 3% value, and this could possibly be increased to reduce the flow rate, for similar reasons.

The laterally distributed depth-averaged velocity, at the apex of the bend, was estimated for a depth of 0.25m (Figure 6.65). The predicted data compares fairly well to the measured data, however, the left floodplain velocities were slightly under-predicted. The total measured flow rate was 0.6139m^3/s and the predicted value was 0.6254m^3/s (i.e. 1.8% different).

The stage-discharge predictions for Series B38 (inbank) and 39 (out-of-bank) are shown in Figures 6.66 and 6.67 respectively. This channel has a higher sinuosity and thus the calibrated C_{uv} values were higher. Furthermore, the main channel cross-section is similar to that of Series B25 and B26, and therefore the C_{uv} values should be increased for similar reasons.

The depth-averaged velocity distribution was predicted for a depth of 0.2m (Figure 6.68), at the bend apex. From this velocity distribution, it is possible to see that on the right of the main channel, the velocity is over-predicted. This is expected as the C_{uv} value is zero on the laterally rising slope (left-right across channel). The solution was to increase the C_{uv} value, hence, on the left of the channel the velocities have been under-predicted to compensate for this. The measured flow rate was 0.1792m^3/s and the predicted flow was 0.183m^3/s (i.e. 2.1% different).

(iii) River Blackwater 1:5 scale model data

The River Blackwater 1:5 scale model was used to predict both discharge and velocities across the channel. Cross-section 5, at the bend apex, was selected due to availability of measured velocities. This was considered for the case of horizontal berms and berms inclined at 1V:30H. These two geometries are depicted in Figures 6.69 and 6.70. The model input parameters are tabulated below (Table 6.12).

Table 6.12 River Blackwater 1:5 scale section 5 model/input parameters

Parameter	**Default Value**	**Value Used**
Reach average longitudinal bedslope S_o	0.001	0.000847
Absolute roughness height k_s (m) (1) main channel (2) floodplain	RA / RHS	 0.014 0.014
Equivalent n_l (1) main channel (2) floodplain	RA / RHS	 0.019 0.019
Colebrook-White equation coefficients (details Table 4.2) (1) laboratory/engineered channel, trapezoidal, smooth (2) laboratory/engineered channel, trapezoidal, rough (3) Real rivers/natural channels		(1)
Main channel dimensionless eddy viscosity (λ_{mc})	0.24	✓
Inbank secondary flow coefficient (Γ_{imc})	+0.050	0
Main channel out-of-bank secondary flow coefficient (Γ_{omc})	+0.150	0
Floodplain out-of-bank secondary flow coefficient (Γ_{ofp})	-0.250	0
Sinuosity σ	0	1.18
Meandering secondary flow coefficient (% C_{uv}) (1) inbank (2) out-of-bank	 0 0	 - 2.5
Temperature of fluid (T °C)	15	✓
Top of bank panel markers present		✓

The stage-discharge data was predicted reasonably well (Figure 6.71), however, the measured data was largely under-predicted just above bankfull. The depth-averaged velocity (Figures 6.72 & 6.73) for depths of 0.187m and 0.237m were predicted. For the lower depth, the velocities corresponded well with the measured values. At the

greater depth, the skew in the main channel was under-predicted. The actual flow rates were 0.082m^3/s and 0.165m^3/s and the predicted values were 0.0825m^3/s (i.e. 0.6% different) and 0.181m^3/s (i.e. 8.8% different).

The depth-averaged velocity prediction at depth = 0.237m for the case with the inclined berms (Figure 6.74) corresponds well with the data. The measured flow was 0.1236m^3/s and the predicted flow was 0.1214m^3/s (i.e. 1.8% different).

(iv) River Blackwater

The River Blackwater was selected in part to test the effects of scale on the model parameters. Cross-section 3 was selected as this has a similar geometry to section 5 in the 1:5 scale model, however, it is situated in the previous meander bend (at the apex) i.e. opposite sign for the C_{uv} coefficient. Figure 6.75 shows the 1997 surveyed geometry (Sellin, 2002). The model parameters are summarised in Table 6.13.

Table 6.13 River Blackwater section 3 model/input parameters

Parameter	**Default Value**	**Value Used**
Reach average longitudinal bedslope S_o	0.001	0.00044
Absolute roughness height k_s (m) (1) main channel (2) floodplain	RA / RHS	 1.360 1.360
Equivalent n_l (1) main channel (2) floodplain	RA / RHS	 0.040 0.040
Colebrook-White equation coefficients (details Table 4.2) (1) laboratory/engineered channel, trapezoidal, smooth (2) laboratory/engineered channel, trapezoidal, rough (3) Real rivers/natural channels		(3)
Main channel dimensionless eddy viscosity (λ_{mc})	0.24	✓
Inbank secondary flow coefficient (Γ_{imc})	+0.050	0
Main channel out-of-bank secondary flow coefficient (Γ_{omc})	+0.150	0
Floodplain out-of-bank secondary flow coefficient (Γ_{ofp})	-0.250	0
Sinuosity σ	0	1.18
Meandering secondary flow coefficient (% C_{uv}) (1) inbank (2) out-of-bank	 0 0	 - -2.5
Temperature of fluid (T °C)	15	✓
Top of bank panel markers present		✓

The stage-discharge measured data shows some degree of scatter, but essentially it describes the rising and falling limb for the rating curve. The Conveyance Generator predicts the average data trend reasonably well. For ideal results, the change in water surface slope for the rising and falling limb is required.

(v) River Severn (upstream of Shrewsbury)

The River Severn cross-section is taken just downstream of a large meander bend, however the study reach is essentially straight. Figure 6.77 shows the cross-section topography. The C_{uv} value has been set to correspond to a sinuosity just greater than 1.1 i.e. only the meandering secondary flow term is in effect. The input parameters are summarised in Table 6.14.

Table 6.14 River Severn upstream of Shrewsbury model/input parameters

Parameter	Default Value	Value Used
Reach average longitudinal bedslope S_o	0.001	0.000146
Absolute roughness height k_s (m) (1) main channel (2) floodplain	RA / RHS	 0.300 0.180 (rfp)
Equivalent n_l (1) main channel (2) floodplain	RA / RHS	 0.031 0.029
Colebrook-White equation coefficients (details Table 4.2) (1) laboratory/engineered channel, trapezoidal, smooth (2) laboratory/engineered channel, trapezoidal, rough (3) Real rivers/natural channels		(3)
Main channel dimensionless eddy viscosity (λ_{mc})	0.24	✓
Inbank secondary flow coefficient (Γ_{imc})	+0.050	0
Main channel out-of-bank secondary flow coefficient (Γ_{omc})	+0.150	0
Floodplain out-of-bank secondary flow coefficient (Γ_{ofp})	-0.250	0
Sinuosity σ	0	>1.1 downstream of large meander
Meandering secondary flow coefficient (% C_{uv}) (1) inbank (2) out-of-bank	 0 0	 - 0.8
Temperature of fluid (T °C)	15	✓
Top of bank panel markers present		✓

Only two measured stage-discharge values were available. Figure 6.78 shows the predicted rating curve. The depth-averaged velocity distribution was predicted for a depth of 7.62m (Figure 6.79). The velocity distribution agrees reasonably well with the measured data. More information regarding the roughness variation across the channel could improve this prediction. The measured flow was 103m^3/s and the predicted flow was 104.73m^3/s (i.e. within 1.65%).

6.3 Conclusion

This section has documented the testing and calibration of the Conveyance Generator against small-scale flume, large-scale flume and purpose-made field measurements. The straight channel flow, velocity and bed shear stress predictions compared well to the observed experimental and field data. The skewed channel stage-discharge was reasonably accurate, however, the C_{uv} coefficient did not capture the higher floodplain velocities on the side in the direction of the skewed velocity profile, as it only applies to the main channel. The meandering results for the stage-discharge correspond well to

the measured data, provided the correct C_{uv} value is allocated. The value of this parameter will be discussed further in Section 7. The depth-averaged velocity predictions for the meandering channels predicted the non-symmetrical effects, although not completely following the data profile.

Overall, the testing of the methods incorporated in the Conveyance Generator have provided good results, that are an improvement on any current 1D approach, and the depth-averaged velocity and bed shear stress lateral distributions will be a by-product of the solution. Section 7 revisits the four calibration coefficients, the sensitivity of the parameters, and it provides a comparison of the results to the 1D hydrodynamic modelling package ISIS.

7. COMPARISON WITH ISIS AND SENSITIVITY TESTING

This section involves comparison of the ISIS conveyance predictions to the measured experimental and field data, as well as to the results of the Conveyance Generator. The sensitivity of the four calibration coefficients is discussed and advice is provided on assigning values to these parameters for different flow conditions. The influence of the reach-averaged longitudinal bedslope on the calculated conveyance is quantified, to provide advice on the accuracy requirement for this parameter.

7.1 ISIS predictions

The stage-discharge curves that were predicted with the Conveyance Generator in Section 6 were calculated with ISIS. Two options were considered:

(i) curves calculated using the calibrated CG local roughness values or n_l
(ii) curves calibrated to achieve the best-fit to the measured data i.e. n_e values

For the initial option (i), the discharge for a given stage is over-predicted, which is expected due to the reduced local friction value (see Figures 7.1 – 7.11 in Appendix 4). The inbank flows were predicted well, while for the overbank flows, where there are increased losses present due to strong secondary currents and turbulence between the main channel and floodplains, the discharge was over-predicted.

For the second option (ii), the ISIS calibrated roughness values incorporate all the energy loss mechanisms e.g. losses due to change in form, expansion and contraction, momentum transfers between the vertical slices and channel sinuosity. Figures 7.12 – 7.22 show the calibrated stage-discharge curves for the same data sets as (i). The Conveyance Generator and ISIS both predict the inbank flow reasonably well, however, the Conveyance Generator predicts the overbank measured flows more accurately, in particular, in the region just above bankfull.

In the Conveyance Generator, the local n_l or absolute roughness dimension k_s, incorporates local friction losses only. Energy losses due to lateral shearing, secondary flows and meandering effects are included in the other calibration parameters i.e. λ, Γ and C_{uv}. The result is that the calibrated '*n*' values determined in Section 7.1.1, are the original Manning's *n*-values, which are all-encompassing (n_e). The stage-discharge curves were thus calibrated for a larger *n*-value, and Table 7.1 provides this comparison. The final column illustrates the amount that *n* was increased to account for the losses other than friction i.e. $n_e - n_l$.

Table 7.1 Comparison of the local n_l used in the Conveyance Generator and the all-encompassing n_e

Channel Section / Series no.	ISIS n_e		CG n_l		Other energy losses in CG			Difference n_e - n_l	
	n_{mc}	n_{fp}	n_{mc}	n_{fp}	λ	Γ	C_{uv}	n_{mc}	n_{fp}
Straight									
FCFA Series 2&4	0.0110	0.0110	0.0087	0.0087	✓	✓		0.0023	0.0023
River Main Sect. 6	0.0360	0.0400	0.0320	0.0340	✓	✓		0.0040	0.0060
River Main Sect. 14	0.0270	0.0350	0.0250	0.0280	✓	✓		0.0020	0.0010
River Severn (Montford)	0.0300	0.0450	0.0300	0.0350	✓	✓		0.0000	0.0100
Meandering									
Glasgow G75T90S	0.0160	0.0160	0.0140	0.0140	✓		✓	0.0020	0.0020
Glasgow G25T45S	0.0160	0.0160	0.0135	0.0135	✓		✓	0.0025	0.0025
FCFB Series B20/21	0.0140	0.0140	0.0110	0.0110	✓		✓	0.0030	0.0030
FCFB Series B25/26	0.0140	0.0140	0.0110	0.0110	✓		✓	0.0030	0.0030
FCFB Series B38/39	0.0160	0.0160	0.0110	0.0110	✓		✓	0.0030	0.0030
Blackwater 1:5 model	0.0240	0.0240	0.0190	0.0190	✓		✓	0.0050	0.0050
River Blackwater	0.0600	0.0600	0.0400	0.0400	✓		✓	0.0200	0.0200

7.2 Parameter calibration

The sensitivity of four calibration parameters, f, λ, Γ and C_{uv} are discussed in this section, together with the impact of the reach-averaged longitudinal bedslope S_o on the predicted conveyance.

7.2.1 Sensitivity of the local friction factor *f*

The Colebrook-White equation is employed for determining the cross-section and depth variations of the local friction factor, f. Details are provided in Section 4.4.2, where three sets of equation coefficients are provided (Table 4.2) for the case of smooth experimental/engineered channels, rough experimental/engineered channels and natural channels respectively. The impact of using these three different equations for a particular channel is considered.

Figure 7.23 & 7.24 show the predicted depth-averaged velocity and local friction factor respectively for a FCFA Series 2 symmetrical flow case, with depth of 0.16873m. It is apparent that the natural channel formula predicts lower velocities, followed by the smooth-engineered option and unexpectedly, the rough-engineered channel predicts higher velocity values. All three equations predict the velocity distribution with reasonable accuracy. The lower velocities in the rough-engineered channel are expected from the distribution of the friction factor, where the values of the friction factor are lower compared to the other two equations. Table 7.2 provides the predicted total flows (m^3/s) and percentage change from the measured value. These values are all within 5%

of the actual value, with the equation for rough-engineered channels providing the nearest prediction.

Table 7.2 Comparison of the total flow rates for the different Colebrook-White equation options (FCFA Series 2 depth of 0.16873m)

Measured Flow	Smooth engineered	Rough engineered	Natural channel	% change from measured data		
				Smooth	Rough	Natural
0.2483	0.2396	0.2418	0.2378	3.5%	2.6%	4.2%

A similar analysis was undertaken for a natural channel, the River Severn at Montford Bridge. Figure 7.25 shows the resulting depth-averaged velocity distributions. Although these vary similarly to those of the previous example, with the rough-engineered channel providing the least conservative estimate, there is little change when compared to the measured data. The flow rates are summarised in Table 7.3, with the maximum change in flow within 1% of the measured value.

Table 7.3 Comparison of the total flow rates for the different Colebrook-White equation options (River Severn at Montford Bridge, depth of 6.92m)

Measured Flow	Smooth engineered	Rough engineered	Natural channel	% change from measured data		
				Smooth	Rough	Natural
229.8	229.56	231.8	227.9	0.1%	-0.9%	0.8%

The results for the sensitivity of f in both experimental and natural channels indicate that the choice of Colebrook-White equation has little influence on the resulting flow predictions. The predicted flow rate is more variable for the experimental flume (5%) than for the natural channel (1%), which is favourable as the CES will essentially be applied to natural channels. This could arise from the larger k_s value in the natural channel causing the roughness term to have a greater role than the viscosity term in the Colebrook-White formulation, and hence less variation.

7.2.2 Sensitivity of the main channel dimensionless eddy viscosity λ_{mc}

The main channel dimensionless eddy viscosity value, λ_{mc}, is the parameter that can be varied in equation (4.14)

$$\lambda = \lambda_{mc}\left(-0.2 + 1.2D_r^{-1.44}\right) \tag{4.14}$$

for determining the amount of lateral diffusion. This value was calibrated on the FCFA data, with particular emphasis on the stage-discharge results. Figure 7.26 shows the impact on the depth-averaged velocity distribution of varying this value between 0 and 0.5. A value in the range 0.1-0.3 captures the curvature of the measured data in the mixing region. A λ_{mc} of 0.24 was found to best-fit this curvature for a range of depths, producing an accurate stage-discharge relationship. Figure 7.27 shows the dimensionless eddy viscosity distributions, which may assume large values in the floodplain regions. Table 7.4 provides a summary of the predicted flow rates, and the percentage change when compared to the measured flow. The value of λ_{mc} = 0.24 is most favourable, providing a flow rate within 0.6% of the measured value. This was the value adopted throughout the study.

Table 7.4 Comparison of the total flow rates for different values of the main channel dimensionless eddy viscosity

Measured flow	CG predicted flow for λ_{mc} of				% change from measured value for λ_{mc} of			
	0.00	**0.13**	**0.24**	**0.50**	**0.00**	**0.13**	**0.24**	**0.50**
0.324	0.341	0.306	0.326	0.319	-5.2%	5.5%	-0.6%	1.5%

7.2.3 The secondary flow term Γ

In straight channels, secondary flows occur for both in and out-of-bank flows. The secondary flow calibration parameter Γ is defined in Section 4.4.4 $[=(1-k)gHS_o]$. There are two sources of discontinuity for this parameter. The first is for over-bank flow, where the coefficient *k* varies for main channel and floodplain flow. The result is a lateral discontinuity at the main channel – floodplain interface. Previous research (Abril, 2001) has found this variation has negligible impact.

The second discontinuity is the change in *k* value at bankfull level. Research to date does not advise on the ideal relative depth for this transition to occur. Figure 7.28 provides the stage-discharge curves for a two-stage channel from the FCFA Series 2 data. The three curves represent one which was determined based on inbank *'k'* value, one based on the overbank *'k'* value and one based on the combination, where the transition is implemented at bankfull termed the CG combined approach. Figure 7.29 provides an enlargement of the bankfull region. It is apparent that in this case, a transition at a depth just above bankfull would have been more favourable i.e. at the intersection of the inbank and overbank curves. These individual curves follow the data more closely than the combined curve, although both are an improvement on any former approach.

7.2.4 Secondary flow terms for meandering channels

For meandering channels of low sinuosity, i.e. in the range 1.0-1.1, the proposed model was to combine the Γ and C_{uv} with a linear relationship, e.g. x times Γ and (1-x) times C_{uv} with x between 0 and 1, would give the total secondary flow loss contribution (details in Section 4.2). To implement this model, it is first necessary to determine the value of C_{uv} for a sinuosity of 1.1.

A regression analysis for the relationship between C_{uv} and sinuosity σ for inbank flow in fully meandering channels, based on the calibrated values from Section 6, has been undertaken. However, only two sinuosities, 1.374 and 2.04 were considered for the inbank flow case. Introducing a third data point i.e. C_{uv} of 0.0 for a sinuosity of 1.0, a regression analysis can be applied to the whole range of sinuosities (Figure 7.30). This does however, exclude the model for the region of sinuosity 1.0-1.1. The R^2 fit is 1.0, and adding an extra data point to the data set that satisfies the regression equation, it can be observed that this curve would imply a rapid increase in C_{uv} for high sinuosities. Alternatively, a straight line can be plotted through the two available data points (Figure 7.31).

For the overbank flow case, more data is available. For the fully meandering condition, i.e. sinuosity greater than 1.1, Figure 7.32 provides a regression analysis. The R^2 fit is

0.9755 which is reasonable in view of the limited data. This regression suggests a value of approximately 1% for a sinuosity of 1.1. Figure 7.33 shows the data for the channels within the range 1.0-1.1 i.e. the data from the FCFA channels skewed at 5 and 9 degrees respectively, along with a single point illustrating that a sinuosity of 1.0 the C_{uv} value is 0.0. This data follows the trend of a slight variation of the proposed model i.e. a linear combination of Γ and C_{uv} in the range $1.0 < \sigma < 1.015$, with a C_{uv} value of 1% at a sinuosity of 1.015. Although the data is scattered about the line, the sinuosity range is small and it is unlikely that the casual user will estimate the sinuosity in this range with great accuracy. The originally proposed model can thus be altered such that:

(i) For straight channels $C_{uv} = 0$

(ii) For inbank flow in channels of sinuosity greater than 1.0, C_{uv} is given by,

$$C_{uv} = 4.3274\sigma^2 - 7.8669\sigma + 3.5395 \tag{7.1}$$

(iii) For overbank flow in channels of sinuosity between 1.0 and 1.015 the secondary flow term is a linear combination of Γ and C_{uv}

(iv) For overbank flows in channels of sinuosity greater than 1.015 the secondary flow term C_{uv} is given by,

$$C_{uv} = 7.1659\sigma - 6.6257 \tag{7.2}$$

This model does require further calibration and testing, however, in view of the current time constraints this model is considered adequate.

7.2.5 Dependence of conveyance on slope

The reach-averaged longitudinal bedslope S_o is an input requirement for the Conveyance Generator. As the primary output is conveyance for a given stage, a sensitivity analysis has been undertaken to determine the accuracy within which this slope should be determined to provide a reasonable estimate of the overall conveyance. The total flow, Q, is determined from the lateral integration of equation (4.8a,b) which have been updated to account for the sinuosity range outlined in 7.2.4, as

$$gHS_o - \frac{f\beta q^2}{8H^2} + \frac{\partial}{\partial y}\left[\lambda H\left(\frac{f}{8}\right)^{1/2} q \frac{\partial}{\partial y}\left(\frac{q}{H}\right)\right] = \frac{(1.015-\sigma)}{0.015}\Gamma + \frac{(\sigma-1.0)}{0.015}C_{uv}\frac{\partial}{\partial y}\left[\frac{q^2}{H}\right]$$

$1.0 = \sigma$ inbank

$1.0 \le \sigma \le 1.015$ overbank

$$gHS_o - \frac{f\beta q^2}{8H^2} + \frac{\partial}{\partial y}\left[\lambda H\left(\frac{f}{8}\right)^{1/2} q \frac{\partial}{\partial y}\left(\frac{q}{H}\right)\right] = C_{uv}\frac{\partial}{\partial y}\left[\frac{q^2}{H}\right]$$

$\sigma > 1.0$ inbank

$\sigma > 1.015$ overbank

(7.3a,b)

The conveyance, *K*, is given by equation (2.3),

$$K = \frac{Q}{S_f^{1/2}} \tag{2.3}$$

where S_f is approximated by S_o. The conveyance for a given channel has been estimated for various slopes, to ascertain the dependency of conveyance on slope. This analysis was undertaken for a FCF Phase A Series 2 & 4. The measured bedslope was 0.001027m/m. The conveyance for this bedslope was compare to that for slopes altered by a factor of ± 2, 1.5, 1.3 & 1.1 % of this value. Figure 7.34 compares the predicted conveyances to that calculated with the correct bedslope. Figure 7.35 provides the percentage change in conveyance when compared to the actual conveyance, for the range of depths. The percentage error is high at low depths and slightly higher just above bankfull. Table 7.5 provides the resulting error bands.

Table 7.5 Percentage change in conveyance with change in bedslope

Bedslope S_o = 0.001027	**factor change in bedslope**	**% change in conveyance**
0.0020540	*2.0	+1.92
0.0015405	*1.5	+1.16
0.0013351	*1.3	+0.77
0.0011279	*1.1	+0.20
0.0009336	/1.1	-0.29
0.0007900	/1.3	-0.82
0.0006850	/1.5	-1.20
0.0005135	/2.0	-2.27

Provided the bedslope can be approximated within 100% (i.e. a factor of two) of the actual value, the predicted conveyance should fall within 3% of the actual value.

7.3 Conclusions

Section 7 has provided a comparison of the conveyance predictions from ISIS and the Conveyance Generator with the measured data. The differences between the all-encompassing Manning's n_e value and the local n_l value have been quantified for these data sets. The sensitivity of the four calibration coefficients *f*, λ, Γ and C_{uv} has been discussed. The choice of factors for the Colebrook-White equation has been found to have negligible impact on the accuracy of the results. A main channel dimensionless eddy viscosity value of 0.24 has adequately represented the amount of diffusion present in the various channel shapes. The lateral and vertical discontinuity of the coefficient k for describing the secondary flow term, Γ, has been found to have little or no influence on the results. The model for the combination of Γ and C_{uv} described in Section 4 has been updated to include a smaller transitional range between straight and fully meandering values i.e. for sinuosities in the range 1.0-1.015. A regression analysis on the calibrated meandering data has provided a guideline for determining C_{uv}, in the absence of further research. The dependency of conveyance on reach-averaged longitudinal bedslope has been considered, and provided the bedslope is estimated within a factor of ±2 of the actual value, the conveyance prediction should be within 3%

or the actual conveyance capacity. A number of research issues have arisen, and these are documented as part of Section 8.

8. CONCLUSION

Interim Report 2 is the designated output for Task T2 of the Targeted Programme of Research being undertaken at HR Wallingford for reducing uncertainty in flood level prediction. The content of this report entails a review of previous research in this area, the conveyance calculation methodology that has been adopted for the Conveyance Generator and the testing of this approach against experimental and real river data. This section provides a brief overview of the report findings.

The conveyance estimation methods that are currently employed in commercially available river modelling software are principally based on historic formulae, with little or no account of recent advances in knowledge and understanding. The conveyance approaches incorporated in the one-dimensional hydrodynamic packages; ISIS, HECRAS and MIKE11 have been reviewed. The calculation approaches are essentially based on a divided channel methodology, which is limited in that the formulae are empirically based, the turbulence generated through shearing between vertical slices and secondary flows is ignored and the main channel and floodplain flows are under and over-predicted respectively. There are further variations in flow estimates with the number of panels representing the section.

A review of the more recent work over the last twenty years identified two key approaches to conveyance: (i) the energy loss method and (ii) depth-integration of the Reynolds-Averaged Navier-Stokes (RANS) equations. The first method was found to be inadequate as it cannot be applied to irregular geometries, it has not previously been tested against real river data, it does not incorporate local variations in bed friction and the energy losses are reach averaged. The RANS approach was favoured as it is physically based, it represents all the energy loss mechanisms, it has been rigorously tested against both laboratory and field data and it has the added advantage of providing the lateral depth-averaged velocity and bed shear stress distributions. It is, however, limited in that it requires the calibration of four parameters, the local friction f, the dimensionless eddy viscosity λ, the secondary flow term Γ and the sinuosity coefficient C_{uv}.

The RANS approach is based on the original Shiono Knight Method (SKM) (Shiono & Knight, 1989) that was extended by Ervine et al (2000) for meandering channels. These two approaches essentially differ in their description of the secondary flow term. The final Conveyance Generator methodology incorporates a combination of these two approaches, where the secondary flow term is varied for straight, skewed and fully meandering channels. The local friction f is determined from the Colebrook-White formulation, the distribution for the dimensionless eddy viscosity λ and the secondary flow term Γ is based on previous research (Abril, 2001) and the coefficient C_{uv} is a function of the sinuosity and relative depth.

The final depth-integrated RANS equations are non-linear, elliptic, second order partial differential equations. A numerical solution technique is adopted, based on the finite element method, which is well suited to the solution of elliptic equations. The cross-sectional area of flow represents the solution domain, which is discretised laterally into a number of elements. A Dirichlet boundary condition is prescribed and the iteration procedure is designed to converge nearly quadratically.

The proposed methodology was tested against physical model data and real river measurements purpose-made for research. The straight channel flow, velocity and bed shear stress predictions compared well to the observed experimental and field data, and the method can thus be implemented with confidence for straight prismatic simple and two-stage channels. The stage-discharge estimated for skewed channels compared well to the measured data. For the depth-averaged velocity profiles, the C_{uv} coefficient did not capture the higher floodplain velocities on the side in the direction of the skewed velocity profile, as it only applies to the main channel. It did, however, predict the skew of the main channel velocities reasonably well. The meandering stage-discharge predictions correspond well to the measured data, provided the correct C_{uv} value is allocated. In particular, the CG predicts the discharge variations just above the bankfull level. The depth-averaged velocity profiles for the meandering channels predicted the non-symmetrical effects, although not following the measured data profile completely.

The stage-discharge relationships for the various channels were also predicted with the one-dimensional hydrodynamic modelling package, ISIS. The results were compared to both the measured data and the CG predictions. In general, the Conveyance Generator curves predict the stage-discharge more accurately, following the exact variations of the measured data. A comparison of the all-encompassing Manning n_e value and the local n_l value is undertaken, to quantify the turbulent and sinuosity effects on the general n-value. In some instances, the increase in n_l due to turbulence from shearing and secondary flows resulted in a 30% increase in the n_l value.

A sensitivity analysis of the four calibration coefficients was undertaken. The selection of the coefficients for the Colebrook-White equation (for solution of the local friction f) was found to have negligible influence on both the depth-averaged velocity profiles and, more importantly, the stage-discharge predictions. A value of the main channel dimensionless eddy viscosity in the range 0.2 and 0.3 was found to predict the lateral diffusion reasonably well, and the value 0.24 was adopted as this provided the best estimate for the stage-discharge relationship. The secondary flow term Γ was considered in terms of the discontinuity at bankfull and on the main channel - floodplain interface. In the latter, a lateral discontinuity, has previously been found to have negligible impact (April, 2002). Although the vertical discontinuity at bankfull provided a 'bump' in the stage-discharge curve, this did not greatly impact the overall curve. The coefficient for meandering, C_{uv}, was quantified for inbank, out-of-bank and low sinuosity flows. A regression analysis for the available calibrated data provides some guidance for the value of C_{uv}. Comparison of the River Blackwater 1:5 scale model and the River Blackwater illustrated that the same value of C_{uv} applies for a similar sinuosity, despite the change in scale.

The dependence of conveyance on slope was evaluated. For the FCF Phase A two-stage channel under consideration, it was found that provided the reach-averaged longitudinal bedslope is estimated within a factor of 2 of the actual value, the resulting discharge prediction should be within 3% of the real value.

The Conveyance Generator provides a vast improvement on the existing one-dimensional conveyance estimation software, however the limitations should be recognised:

(i) The semi-2D approach does not capture the 3D-flow behaviour observed with main channel – floodplain interaction, particularly in meandering channels. In instances where the floodplain may act as a series of ponds with lateral flows between the main channel and floodplain, a 1D hydrodynamic model is preferable, where the conveyance is calculated in the main channel only. The floodplains could hence be modelled as a series of reservoirs with lateral spills from the main channel or a similar option.

(ii) A full 3D model would be ideal for representing the more complex flow behaviour e.g. main channel-floodplain mixing, flow around structures/bed features/vegetation, 3D spirals generated through meandering etc. 3D models are, however, computationally more expensive, require a model for the free surface and may provide excess data in areas where the local flow features are not required. 3D models are thus not a recognised alternative in the foreseeable future.

(iii) Further aforementioned limitations include evaluating the four calibration coefficients for the RANS approach, together with the contributions from the straight and meandering secondary flow effects.

The depth-integrated RANS methodology outlined and tested within this report satisfies the criteria cited in the Terms of Reference (Section 1.2):

"Develop selected method(s) to cover all cases of river/floodplain morphology. Ideally there should be a single unified method, with mechanism related terms which drop out or take zero values in various cases, determined by the measurable river system parameters mentioned above."

This approach is based on recent research, expert guidance and in part, the result of the final model calibration. It provides a substantial improvement on previous historic/hand-calculation approaches to conveyance and has the added advantage of providing velocity and bed shear stress distributions, which are critical to vegetation cutting and sediment transport respectively. As the model incorporates four calibration parameters, there is some degree of uncertainty about the exact description of these parameters. Section 9 thus provides recommendations for possible future research, which may be incorporated within the Strategic Programme.

9. RECOMMENDATIONS

This section lists recommendations for future research, which may be incorporated within the Strategic Programme.

(i) Section 7 identified the discontinuity of the secondary flow term Γ across lateral boundaries i.e. the floodplain – main channel interface. This parameter should be modelled for straight prismatic two-stage channels such that there is no abrupt change between the positive main channel value and the negative floodplain value. This model should be extended to cover all possible case e.g. braided channels.

(ii) Section 7 identified the discontinuity of the secondary flow term Γ across the vertical boundary i.e. at bankfull. This parameter should be modelled for straight prismatic two-stage channels such that there is no abrupt change between the small positive value for inbank flow (small secondary flows) and the larger positive value for overbank flows (larger and more complex secondary flows). The model could possibly vary as a function of the relative depth, due to the complex variations in secondary flow orientation with depth (details in Section5.3.2).

(iii) A simple model for combining the secondary flow term Γ and the meandering coefficient C_{uv} for the range of sinuosities 1.0-1.015 has been proposed. A more robust model for this relationship should be developed, based on the calibration of a large number of skewed and gently meandering channels.

(iv) A regression analysis to determine the value of C_{uv} for both in and out-of-bank flow cases has been undertaken. This should be carried out with a comprehensive data set consisting of both physical model and real river data.

(v) A model should be developed for the variation of C_{uv} in the transition from in to out-of-bank flow i.e. where the value of C_{uv} abruptly changes sign to compensate for the change in orientation of the skewed velocity profile/water surface elevation.

(vi) An analysis the value of C_{uv} at different sections through a meander bend should be undertaken e.g. at the bend apex, the crossover section and straight sections downstream of complex bends.

(vii) An alternative approach to combining the secondary flow term Γ and the meandering coefficient C_{uv} could be developed, where only the C_{uv} term is implemented. For straight prismatic channels, the C_{uv} term would be applied symmetrically as a function of the lateral bedslope S_y. This would imply a change in sign for the C_{uv} term at the centre of the main channel for straight prismatic channels. The result would be a symmetrical reduction in the overall unit discharge/depth-averaged velocity profiles, thus reducing the total flow rate through incorporating the energy losses due to the secondary flows in straight channels.

(viii) A further alternative for meandering channels could be to implement an energy loss approach, where the channel is subdivided into zones within which particular flow processes occur. This would require extending the method to channels with natural geometries and conversion of the reach-averaged flow parameters to a cross-sectional framework.

10. REFERENCES

Abril B., 2001, Updated RFMFEM Finite Element Model based on the SKM for Depth-averaged River Flow Simulation, *EPSRC Technical Report* GR/R54880/01.

Ackers P., 1992, Hydraulic Design of Two-Stage Channels, *Proc. ICE Journal for Water, Maritime and Energy*, Paper no. 9988, Vol. 96, Dec., pp 247-257.

Ackers P., 1993, Stage-discharge Functions for Two-Stage Channels: The Impact of New Research, *Journal Institute Water and Environmental Management*, Vol. 7, No. 1, February, pp 52-61.

Ackers P., 1993, Flow Formulae for Straight Two-Stage Channels, *Journal of Hydraulic Research*, IAHR, Vol. 31, No. 4, pp 509-531.

Ackers, 1958, Resistance of Fluid Flows in Channels and Pipes, *Hydraulics Research Paper*, No. 1, HMSO, London.

Babaeyan-Koopaei, K., Ervine, D.A., Carling P.A. & Cao Z., 2002, Velocity and Turbulence Measurements for two Overbank Flow Events in River Severn, *Journal. of Hydraulic Engineering*, Vol. 198, no. 10, October i.e. as yet unpublished.

Barr D.I.H., 1975, Two Additional Methods of Direct Solution of the Colebrook-White Function, *Proc. Inst. of Civil Engineers*, vol. 59, pp 827.

Bousmar D. & Zech Y., 1999, Momentum Transfer for Practical Flow Computation in Compound Channels, *Journal of Hydraulic Engineering*, ASCE, Vol. 125, No. 7, July, pp 696-706.

Bousmar D., 2002, Flow Modelling in Compound Channels: Momentum transfer between main channel and prismatic and non-prismatic floodplains, PhD Thesis, *Universite Catholique de Louvain*.

Chang H.H., 1983, Energy Expenditure in Curved Open Channels, *Journal of Hydraulic Engineering*, Vol. 109, No. 7, pp 1012-1022.

Chow V.T., 1959, *Open Channel Hydraulics*, McGraw-Hill Book Company, US.

Colebrook C.F. and White C.M., 1937, Experiments with Fluid Friction in Roughened Pipes, *Proc. Roy. Soc.* , A161, 367.

Cunge J. A., Holly F.M. & Verwey A., 1980, *Practical Aspects of Computational River Hydraulics*, The Pitman Press, Bath.

Davies A.J., 1980, *The Finite Element Methods – A First Approach*, Clarendon Press, Oxford.

Einstein H.A. & Banks R.B., 1950, Fluid Resistance of Composite Roughness, *Trans. American Geophysical Union*, Vol. 31, no. 4, pp 606-610.

Engelund F., 1966, Hydraulic Resistance of Alluvial Streams, *ASCE*, Vol. 92, No. Hy. 2.

Ervine D.A. & Ellis J., 1987, Experimental and Computational Aspects of Overbank Floodplain Flow, *Transactions of the Royal Society of Edinburgh: Earth Sciences*, Vol. 78, pp 315–475.

Ervine D.A., Babaeyan-Koopaei K. & Sellin H.J., 2000, Two-dimensional Solution for Straight and Meandering Overbank Flows, *Journal of Hydraulic Engineering, ASCE*, Vol. 126, no. 9, September, pp 653-669.

Falconer R.A. & Lin B., 1997, Three-dimensional Modelling of Water Quality in the Humber Estuary, Water Research, *IAWQ* 31(5).

HECRAS, 1998, River Analysis System: Hydraulic Reference Manual Version 2.2, U.S. Army Corps. of Engineers, Hydrologic Engineering Center, Davis.

Hydrological Data UK, 1998, Hydrometric Register and Statistics 1991-95, *Institute of Hydrology*, British Geological Survey.

Interim Report 1: Data Mining, 2002, Project W5A, *Report SR 597, HR Wallingford Ltd*, prepared for EA and DEFRA.

ISIS V2.0, 2001, Online Help Manual, Copyright HR Wallingford Ltd. / Halcrow.

James C.S. & Wark J.B., 1992, Conveyance Estimation for Meandering Channels, *HR Wallingford Ltd. Report SR 329*, pp 1-91.

Knight D.W. & Abril J.B., 1996, Refined Calibration of a Depth-averaged Model for Turbulent Flow in a Compound Channel, *Proc. Instn. Civil Eng., Water, Maritime and Energy*, London, Vol. 118, pp 151-159.

Knight D.W. & Shiono K., 1990, Turbulence Measurements in a Shear Layer Region of a Compound Channel, *Journal of Hydraulic Research*, IAHR, Vol. 28, No. 2, 1990, pp 175-196.

Knight D.W. & Shiono K., 1991, Turbulent Open-channel Flows with Variable Depth across the Section, *Journal of Fluid Mechanics*, Vol. 222, pp 617-646.

Krisnamurthy M. & Christensen B.A., 1972, Equivalent Roughness for Shallow Channels, *Journal of Hydraulics Division, ASCE*, Vol. 98, HY12, pp 2257-2262.

Lotter G.K., 1933, Considerations on Hydraulic Design of Channels with Different Roughness of Walls, *Trans. All-Union Scientific Research Institute of Hydraulic Engineering*, Leningrad, Vol. 9, pp 238-241.

Microsoft Visual Basic Version 6.0, 2000, *Microsoft Corporation*.

MIKE11 V3.11, 1995, General Reference Manual, 1st edition, *Danish Hydraulic Institute*.

Muto Y., 1997, Turbulent Flow in Two-stage Meandering Channels, PhD Thesis, University of Bradford.

Muto Y., Shiono K. & Imamoto H., 1998, Three-dimensional Flow Structure in Meandering Channels for Overbank Flow, *Journal of Hydroscience and Hydraulic Engineering*, Vol. 16, No. 1, pp 97-108.

Newton I., 1664-1671, *Methodus fluxionum et serierum infinitarum*.

Nikuradse J., 1933, Translates to: Laws of Flow in Rough Pipes, *Verein deutscher Ingenieure, Forschubgsheft*, No. 361, Berlin.

Pavolovskii N.N., 1931, On a Design for Uniform Movement in Channels with Non-homogenous Walls, *All-Union Scientific Research Institute of Hydraulic Engineering*, Leningrad, Vol. 3, pp 157-164.

Raudkivi A.J., 1998, *Loose Boundary Hydraulics*, A.A. Balkema, Rotterdam, Netherlands.

Samuels P.G., 1989, Some Analytical Aspects of Depth Averaged Flow Models, *Intl. Conf. Hydraulic and Environmental Modelling of Coastal, Estuarine and River Waters*, Bradford, England, 19-21 September.

Scoping Study, 2001, Scoping Study for Reducing Uncertainty in River Flood Conveyance, *R&D Technical Report to DEFRA/Environment Agency*, HR Wallingford Ltd. (Prepared by EP Evans, G Pender, PG Samuels, M Escarameia)

Scoping Study Annex, 2001, Conveyance in 1-D River Models, Prepared by D.W. Knight.

Scoping Study Annex, 2001, The Role Experimental and Field Data, Prepared by A. Ervine.

Sellin, R.H.J. & van Beesten D.P., 2002, Berm Vegetation and its Effect on Flow Resistance in a Two-Stage River Channel: An Analysis of Field Data, *Proceedings of the River Flow 2002 Conference*, Belgium, Zwets & Zeitlinger, Lisse, ISBN 90 5809 509 6, Volume 1, pp 319-327.

Shiono K. & Knight D.W., 1989, Two-Dimensional Analyical Solution Compound Channel, *Proc. 3rd International Symposium on Refined Flow Modelling and Turbulence Measurements*, Universal Academy Press, pp 591-599.

Shiono K. & Knight D.W., 1990, Mathematical Models of Flow in Two or Multi-Stage Straight Channels, *International Conference on River Flood Hydraulics*, Paper G1, pp 229-238.

Shiono K. & Muto Y., 1998, Complex Mechanisms in Compound Meandering Channel with Overbank Flow, *Journal of Fluid Mechanics*, Vol. 326, pp 221-261.

Shiono K., Muto Y., Knight D.W. & Hyde A.F.L., 1999, Energy Losses due to Secondary Flow and Turbulence in Meandering Channels with Overbank Flow, *Journal of Hydraulic Research*, IAHR, Vol. 37, No. 5, pp 641-664.

Toebes G.H. & Sooky A.A., 1967, Hydraulics of Meandering Rivers and Floodplains, *Journal of Waterways and Harbours Division ASCE*, Vol. 93, pp 213-236.

U.S. Army Corps of Engineers, 1956, Hydraulics Capacity of Meandering Channels in Straight Floodways, Technical Memo 2-429, *Waterways Exp. Station*, Vicksburg, Missouri.

Wark J. B., 1993, Discharge Assessment in Straight and Meandering Channels, PhD Thesis, University of Glasgow.

Zienkiewick O.C., 1977, *The Finite Element Method*, 3rd Edition, McGraw-Hill book Company Ltd., UK.

Appendix 1 Derivation for the depth-integrated Reynolds-Averaged Navier-Stokes equations

Appendix 2 Flowchart of the Conveyance Generator program structure

Appendix 3 Results of the Conveyance Generator testing against physical and real river measurements

Appendix 4 Results of the ISIS predictions and sensitivity analysis